ELECTRICAL PROPERTIES OF GLASS - CRYSTAL - METAL COMPOSITES

A Thesis Submitted
In Partial Fulfilment of the Requirements
for the Degree of
MASTER OF TECHNOLOGY

By

DEBASIS ROY

to the
MATERIALS SCIENCE PROGRAM
INDIAN INSTITUTE OF TECHNOLOGY KANPUR
AUGUST, 1982

CERTIFICATE

Certified that this work on 'ELECTRICAL PROPERTIES OF GLASS-CRYSTAL-METAL COMPOSITES' by Mr. Debasis Roy has been carried out under my supervision and that it has not been submitted elsewhere for a degree.

D Chakravorty

(D. CHAKRAVORTY)
Professor
Materials Science Programme
Indian Institute of Technology,
Kanpur.

ACKNOWLEDGEMENTS

I am happy to express my heartfelt gratitude to Professor D. Chakravorty for his excellent guidance, lively suggestions and constant encouragement throughout the course of my work.

The financial assistance given by DST in supporting this investigation is gratefully acknowledged.

I extend my thanks to Mr.B.Sharma, Mr.A.Agnihotri, Mr.S.Das, Mr. I.D. Sharma, Mr. Narsingh, Mr.I. Sharma and Mr. Prasad for their help during my project work.

I thank all my friends & colleagues for their valuable help.

In the last but not the least, I am thankful to Mr.U.S. Misra for his excellent typing.

-Debasis, Roy

I.I.T. Kanpur

August, 1982.

CONTENTS

CHAPTER 1

INTRODUCTION

Glass metal microcomposites consist of a glass phase containing a distribution of metallic particles having dimensions of the order of a few hundred angstroms. The metallic particles may be precipitated either during melting, controlled cooling of the melt or during subsequent heat treatment depending on the glass compositions and melting conditions. The applications of glass metal microcomposites may be broadly classified as follows[1].

1. Photosensitive glasses
2. Photosensitively nucleated glass-ceramics
3. Photochromic glasses
4. Polychromatic glasses
5. Photothermal conversion (cermet)
6. Solar control coatings (electro float process)

Some of the other possible applications will be :

1. Electro-conducting glasses and fibers
2. Memory switching
3. High strength glasses and fibers.

1.1 DEVELOPMENT OF HIGHLY CONDUCTING LAYERS IN GLASS

A number of methods have been developed to obtain a highly conducting layer on or within the surface of the glass. These can be divided into two broad categories. In the first,

the layer is simply applied on to the surface of the glass. Platinum, gold[2] or copper salts are heated to reduction on the surface, metals are vaporised on to the surface[3], silver oxides and metal powders are fired on with the help of auxiliary fluxes and lacquers containing suspensions of flaky metals[4] are applied. The second category involves techniques whereby various glasses containing lead oxide and other metal oxides are reduced in hydrogen gas to induce a conducting layer within the glass surface, which have been developed by Green and Blodgeet[5,6]. They have treated various glasses containing lead oxide and other metal oxides in hydrogen gas and obtained surface resistance which varies from 10^2 ohm/cm^2 to 10^4 ohm/cm^2. The surface resistance value depends on the compositions of glasses chosen.

1.1.1 Ion Exchange and Reduction Technique:

Chakravorty[7,8] has developed a distinct technique by which a highly conducting surface can be induced within the surface of an alkali containing silicate glass and this conducting film is an integral part of the glass system itself. However, one precondition of inducing highly conducting thin film is that the glass surface should be sufficiently rough. The method can be briefly outlined as follows.

After making the glass surface sufficiently rough by grinding off with -120 mesh SiC powders the sample is dipped into molten $AgNO_3$ at about 330°C and $Na^+ \rightleftharpoons Ag^+$ ion exchange

takes place. After the ion exchange treatment a part of Na^+ ions in the thin film of glass surface is replaced by Ag^+ ions. The Ag^+ ions diffuses to the interior of the bulk glass and Na^+ ions come to the surface again and gets ion exchanged with Ag^+ and this process continues. The next step is to reduce the Ag^+ ions by hydrogen gas in the temperature range of 250°C to 400°C. Obviously the surface resistance that will be developed will depend on temperature and time of ion exchange and reduction treatment and it is also expected that it will depend on the surface roughness. Chakravorty observed a surface resistance of the glass, subjected to above mentioned treatment in the range of 0.15 ohm/sq.cm. to 4.1 ohm/sq.cm. By a detailed microstructural analysis of virgin glasses as well as the glass after ion exchange and reduction treatments, he came to the conclusion that the conducting layers in the glasses consist of continuous chains formed by metallic droplets of silver and bismuth respectively. It is believed that during reduction treatment the metallic Ag atoms which are formed by reduction are nucleated at the potential heterogenous sites followed by growth. The potential nucleation sites are provided during the surface grinding of the sample. Due to this surface roughness it was not possible to measure the thickness of conducting film. It has been shown by Das et.al.[9] that the ceramised $CaO-SiO_2-Na_2O-Bi_2O_3$ systems develop high surface conductivity when they are ion exchanged in molten silver nitrate followed by reduction in hydrogen gas. The typical surface resistance varies in the range of 0.08 ohm/sq.cm to 14.76 ohm/sq.cm. depending

on the compositions and reduction temperature and time. Das[10] has shown that the interface between the glass and crystal provides the potential site for the Ag metal to nucleate and grow during reduction treatment. Hence, surface roughness is not necessary in this process of generating highly conducting layer.

In certain amorphous systems, when an applied electric field to the sample crosses a certain critical value the sample goes from a high resistance state to a low resistance state. This phenomenon is known as switching. There are two types of switching-threshold and memory. When the applied electric field is removed the threshold switch reverts back to the off-state. On the other hand the memory switch remains in the on-state even after the removal of the electric field. Alkali borosilicate glasses containing bismuth oxide when subjected to ion-exchange in molten silver nitrate followed by a reduction in hydrogen are found to have microstructure consisting of metallic particles distributed in a glassy matrix. This system[11] is found to exhibit memory switching with a reduction of resistance of six orders of magnitude when the applied electric field crosses the critical value of 30 V/cm. When a 5-volt pulse of 10 msec. duration is applied to the sample it goes from the off to the on-state. However, on application of a 50-volt pulse of 10 msec. duration the sample switches back to the off-state. These glasses have been evaporated in a vacuum of 10^{-5} torr on to alumina substrates to form thin films of a few micron thickness. Such films[12] also show memory switching. When

the sample in the on-state is heated above a temperature (around the melting point of bismuth metal) it reverts from the on to the off-state. Recently, V_2O_5 - P_2O_5 glasses[13] containing metallic bismuth or silver have been reported to show memory switching. The memory switching action has been explained on the basis of a particle stretching model[14].

1.2 CERAMISATION OF GLASSES

Glass ceramics are polycrystalline materials, which are produced from glasses by controlled crystallization. Although some 200 years ago. Reaumer, a French chemist produced a polycrystalline material from the bottle glass by heating it to redness for several days, a true glass ceramic was produced when Stookey[15] of Corning glass in 1947 discovered that a polycrystalline material was produced by heating a photosensitively opacified glass. In the latter case controlled crystallization is possible. This controlled crystallization involves two steps-nucleation and growth. However in the formation of polycrystalline glass ceramics the more important and critical step is nucleation. Because irrespective of the growth rate we are going to get fine grained glass ceramics if the nucleation rate is high and vice versa. So we will put emphasis on the nucleation process.

There are two types of nucleation. They are (a) homogeneous nucleation and (b) heterogeneous nucleation.

1.2.1 Homogeneous Nucleation:

In a phase transformation, when one product phase is nucleated in a parent phase in absence of or without the help of foreign particles it is called homogeneous nucleation, whereas in heterogeneous nucleation the new phases are formed on third phase of different chemical compositions.

The general equation for the rate of homogeneous nucleation given by Becker[16] is as follows:

$$I = A \exp - \frac{(\Delta F^* + Q)}{kT} \qquad (1.1)$$

where

I = Nucleation rate

A = Constant

ΔF^* = Critical free energy change for the formation of nuclei

Q = Activation energy for diffusion

k = Boltzmann constant.

ΔF^*, as a function of surface free energy σ, volume free energy change (Δg) for spherical nuclei is given by the expression,

$$\Delta F^* = \frac{16}{3} \frac{\pi \sigma^3}{(\Delta g)^2} \qquad (1.2)$$

Since Δg is zero at the equilibrium transformation temperature, from equations (1.1) and (1.2) one can see that nucleation rate passes through a maximum in the temperature

range of transformation temperature to 0°K. Hence one can suitably choose a nucleation temperature and can have a particular size of the crystal in the ultimate glass ceramic product. The preparation of glass ceramics by the homogeneous nucleation and growth is rare. However, Strand and Douglas[17] have studied the ceramisation of SiO_2-CaO-Na_2O system in which they observed homogeneous volume nucleation. Burnett and Douglas[18] also observed homogeneous nucleation in Na_2O-BaO-SiO_2 system.

1.2.2 Heterogeneous Nucleation:

The rate of heterogeneous nucleation, given by Turnbull[19] is as follows:

$$I_c = A' \exp - \frac{(\Delta F_c^* + Q)}{kT} \qquad (1.3)$$

where,

$$\Delta F_c^* = \Delta F^* f(\theta) = \Delta F^* \frac{(2+\cos\theta)(1-\cos\theta)^2}{4} \qquad (1.4)$$

and $\cos\theta$ is related by,

$$\sigma_{HM} = \sigma_{PH} + \sigma_{PM} \cos\theta \qquad (1.5)$$

θ is the contact angle of new phase developed relative to third phase and this is related to interfacial tensions of three phases - parent (M), product (P) and third phase (H) as given by equation (1.5). Because of the fact that $f(\theta)$ is fraction for $0° < \theta < 180°$, $I_c > I$.

In the light of equations (1.1) to (1.5) we can come to the following conclusions related to selection of effective catalyst as summarised by Berezhnoi[20] after Stookey:

(1) Low critical free energy change of homogeneous nucleation from melt and this is made possible by the low interfacial energy between the melt and the crystalline phase.

(2) At low temperature the activation energy barrier to diffusion process should be small.

(3) A low interfacial energy should exist between the glass and the nucleation catalyst for effective wetting.

(4) The disregistry of lattice parameters between the crystallising material and the nucleation catalyst should be small and the permissible disregistry is 15%.

(5) High solubility of nucleation catalyst at the melting temperature and limited solubility at low temperature where nucleation and growth of the primary phase occur.

The last criterion is not related to the equations (1.1) to (1.5) but it is obvious, otherwise no heterogeneous nucleation can occur.

In the above discussion of the characteristics of the catalysed crystallization it has been assumed that the first stage in the process is the separation of the submicroscopic crystalline particles. This is highly probable that in the case of metallic nucleation catalyst, the separation of tiny crystals of metals from glass is a precursor to nucleation

and growth of the primary phase on these metallic tiny crystals which act as heterogeneous sites. There is still another route of crystallisation, especially important for oxide catalysts and was discovered by Stookey[21]. The glass forms a homogeneous liquid in the molten state but separates into two immiscible phases during cooling. This phase separation subsequently catalyses the crystallisation. So we see that there are two ways of catalysed crystallisation:(1) nucleation by precipitation of metals and (2) nucleation by two phase separation.

(1) Nucleation by separation of metals:

We have already considered the criteria of selecting such catalysts. However the processes involved can be summarised as follows with copper as an example. The details of these processes for metals like Cu, Ag, Au are given by Mcmillan[22].

(i) Cu is reduced from its ionic state to atomic state and remains uniformly dissolved in the molten glass. If this glass cools fairly rapidly it remains in the glassy state after cooling to room temperature.

(ii) Reheating of the glass leads to formation of the aggregates of copper atoms and these are of submicroscopic dimensions. These aggregates then act as heterogeneous sites on which the primary crystallization occurs by subsequent heat treatment.

(2) Nucleation by two phase separation:

There are two basic reasons for phase separation. The first one is related to geometrical consideration. If the triangular or tetrahedral structure of network formers significantly differs in size than that of SiO_4 tetrahedra, then in accommodating these network formers the SiO_4 tetrahedra will be highly distorted and this will then lead to the phase separation to achieve low energy state.

There is another possible mode of phase separation which also depends on geometrical factor. An ion, for example which assumes tetrahedral coordination at high temperature can take part in tetrahedral network forming groups. But on cooling if it tends to assume octahedral coordination number, this type of structural group will be incompatible with the principal SiO_4 tetrahedra. As a result phase separation will occur.

The second basic reason for the phase separation is the difference between the charge of the principle network forming ion (silicon) and other network forming ions. For example, if the other network forming ion possesses charge +5 then from the electroneutrality condition one of the oxygen ions surrounding the pentavalent ion will be doubly bonded. Due to the asymmetry of these tetrahedral structures there will exist a marked disturbance in the Si-O-Si bonds and this will lead to phase separation. Another important thing in the phase separation is the field strength of the cations which

are accommodated in the holes existing between SiO_4 tetrahedral units. The arrangement of the O^{-2} ions in glasses is mainly determined by the forces exerted by the Si ions. But depending on the field strength of the interstitial cations, they may also influence the O^{-2} arrangements. Thus for the cation of high field strength they will influence to achieve their equilibrium state of coordination. As a result the Si-O-Si bonds will be greatly disturbed and this will lead to phase separation, one phase being rich in SiO_2, to achieve lower free energy state.

The two-phase liquid or glass separation is started by a process of homogeneous nucleation and this is much more likely to occur than homogeneous nucleation of the crystalline phase from the melt. The reason is that the interfacial energy between the two glassy or liquid phases is very small compared to that of the crystalline phase and the melt.

Usually in two phase separation one phase takes the form of droplets and the droplets are uniformly distributed in the matrix of second phase. This droplet may be homogeneously nucleated and then acts as a heterogeneous site for the subsequent crystallization of the matrix. The work of Maurer[23] on $MgO-Al_2O_3-SiO_2$ system with TiO_2 as a nucleating catalyst indicates two phase separation. The droplet phase is one which contains an excess of TiO_2.

From the study of optical scattering he showed that anisotropy of the emulsion or droplet phase increases when heat treated in the temperature range of 725-770°C. This isotropic to anisotropic change is related to the crystallisation of the droplet phase. Devekey and Majumdar[24] also observed homogeneous two liquid phase separation in $MgO-Al_2O_3-SiO_2-CaO$ system containing 8-13% TiO_2. Subsequent heating leads to the formation of pseudobrookite crystallites in the amorphous phase containing excess of TiO_2 (emulsion phase) and these crystallites then act as heterogeneous sites for the subsequent crystallization of a series of metastable phase culminating in α-cordierite.

The other mechanism is the crystallization of the matrix phase, after two phase separation. Hing and Mcmillan[25] have shown in Li_2O-SiO_2 system using P_2O_5 as the nucleation catalyst, by electron microscopic studies that crystallisation occurs in the glassy matrix between the phase separated droplets. They have explained that it is probably due to the P_2O_5 which reduces the interfacial energy (σ) between the crystalline phase developed and the phase separated glassy matrix.

Another possibility is that the interface between the two phase separated phases may act as a heterogeneous site for the heterogeneous nucleation and subsequent crystallisation of the glassy matrix to form glass ceramics. Ohlberg et.al.[26] confirmed that crystal nucleation starts at the glass-glass interface in $Li_2O-CaO-TiO_2-SiO_2$ and in $Li_2O-MgO-Al_2O_3-SiO_2$ glasses. Tomozawa[27] on the basis of optical microscopy and

X-ray small angle scattering measurements on Li_2O-SiO_2 system has come to the same conclusion. Kzumasa et.al.[28] making use of nucleation and growth rate theory has arrived at the same conclusion. However, Harper et.al.[29] and Nakagawa et.al.[30] did not find any supporting evidence in the study of the Li_2O-SiO_2 system.

Homogeneously nucleated crystallisation of matrix phase followed by the crystallisation of droplet phases is also possible. However, this will be lead to the formation of less fine grained glass-ceramics.

In addition to the various mechanisms already discussed, there is another possible effect in catalysed crystallisation which must be mentioned. As we have already seen that (equations (1.1) and (1.2)) interfacial energy between the crystalline phase and the melt constitutes a barrier to nucleation, so it is expected that if by some means the interfacial energy can be reduced, the nucleation rate will be higher. Lowering of interfacial energy will occur, if surface active agents become concentrated at the solid-liquid interface. Hilling[31] has discussed this possibility.

1.2.3 Growth:

We have already mentioned that nucleation is more critical in ceramisation process but it is important to mention here that sometimes the two phase separation has considerable effect on the crystal growth. Tomozawa[32] has shown that in

Li_2O-SiO_2 system, the shift of matrix composition due to phase separation has large effect on crystal growth rate. He has explained the observed difference in the apparent activation energy of the crystal growth by the shift of matrix composition due to phase separation.

So from the discussion of nucleation and growth we may come to the conclusion that in ceramisation what particular mechanism will be involved depends on the system chosen and the kind of nucleating agent added.

1.3 CHOICE OF GLASS SYSTEM

Ceramisation of SiO_2-ZnO-Li_2O-P_2O_5 system has been studied by Macmillan[22]. The phosphorous penoxide acts as a nucleant. If zinc silicate phase can be grown in the glassy matrix, the matrix will become relatively open as the lithium ions are left unexpensed. We may therefore, expect that there will be a decrease in resistivity. Furthermore, the lithium ions can be ion exchanged with silver which on reduction will give a conducting layer. On these expectations we have chosen this system.

1.4 DEVELOPMENT OF HIGH SURFACE CONDUCTIVITY IN GLASS-CERAMICS

In the development of high surface conductivity within the surface of a glass by ion exchange and reduction treatment it is necessary to have rough glass surface. As we have mentioned earlier this rough surface provides the potential sites for the silver metals to nucleate and grow during reduction treatment. Now if a glass is partially ceramised then the glass crystal interface may provide the heterogeneous site (like the rough surface in case of glasses) for the Ag metal to nucleate and grow. So the surface roughness can be completely avoided. Thus by subjecting a glass ceramic to ion exchange and reduction treatment as described later, we can produce a highly conducting glass ceramic surface.

CHAPTER 2

STATEMENT OF THE PROBLEM

An important requirement of the material used as the resistor in potentiometer is that the resistance should be essentially constant around the room temperature. Therefore the temperature coefficient of resistance of the material should be very small i.e., 100 ppm/°K in the temperature range -100°C to + 100°C. In case of wire wound potentiometer the wire may be erroded by friction with contact terminal in course of use, making the instrument useless. The last problem may be circumvented by applying a thin film on an insulating substrate. The TCR of this thin film should be obviously small. One problem associated with applying a thin film on a substrate is that unless the bonding between the thin film and the substrate is sufficiently strong at the interface, the thin film will come out in course of time. Therefore the thin film should be a part of the insulating material and it should be smooth enough to enable the contact terminal to slide over it.

Chakravorty[8] developed highly surface conducting glasses by ion-exchange and reduction treatment. The surface resistances for the samples are in the range of 0.15 ohm/square to 4.1 ohm/square and the TCR is around 2000 ppm/°K. But the necessary precondition is to roughen the surface to 120 mesh.

Reddy[33] developed a high surface conductivity in optically polished (1 micron) glass ceramics by ion exchange and reduction technique and Das[10] developed the same with more polished surface (0.05 micron). In above cases conducting layers formed one integral part of the insulating substrate. The objectives of the present study are the following:

1. To study the nucleation and growth temperatures of glasses of different compositions by DTA technique and to study the composition by ceramising the glasses at different heat treatment temperatures for comparison purpose.
2. To identity crystalline phases by X-ray diffraction.
3. To study the effect of different phases and temperature on the DC and AC resistivity of the glasses.
4. To study the time-temperature effect of ion exchange and reduction on the bulk resistivity of the ion exchanged and reduced glasses.
5. To correlate the bulk resistivity with the amount, sizes and nature of crystals during ceramisation.
6. To find the thickness of the conducting layers of the ion exchanged and reduced ceramised glasses.
7. To study the AC resistivity of un ion exchanged glass at different temperatures.
8. To study the mechanism of conduction.

CHAPTER 3

EXPERIMENTAL PROCEDURE

3.1 PREPARATION OF GLASS

The three glass compositions, under investigation are given in Table 3.1. The glasses have been prepared from reagent grade chemicals. Required quantities of chemicals corresponding to 150 gms of a batch [Appendix 1] are weighed in a physical balance and then mixed with acetone thoroughly in a mortar to achieve a proper homogeneous mixture. For refining 0.2% by weight of As_2O_3 is added.

The dried mixture is transferred to alumina crucible and heated electrically in a furnace fitted with globar rods. After the slow heating in the range of 900°C-1200°C, the final melting is accomplished in the range of 1400°C-1450°C.

After melting, the molten glass is cast in an aluminum mold and annealed for one hour in the temperature range 450°C-500°C and then left for furnace cooling.

3.2 CERAMISATION OF GLASS

3.2.1 Differential Thermal Analysis (DTA), Thermogravimetry (TG) and Derivative Thermogravimetry (DTG):

Normally any phase transformation occurs by a process of nucleation followed by growth at higher temperature. The same is true for the ceramisation of glass. So before ceramisation one should know the nucleation and growth temperature.

TABLE 3.1

Composition of Glasses

Glass No.	Composition in mole %			
	SiO_2	ZnO	Li_2O	P_2O_5
1	60	14	25.2	0.8
2	55	12	32.2	0.8
3	60	19	20.2	0.8

Glass No.	Composition in weight for 150 gm. glass			
	SiO_2	ZnO	Li_2O	P_2O_5
1	96.27	30.47	49.87	5.65
2	92.41	27.35	66.73	5.92
3	92.05	39.55	38.22	5.40

This is actually accomplished by the DTA and the information is complemented by the TG and the DTG analysis.

The principle of DTA technique is to measure the changes in heat content as a function of difference in temperature existing between the sample under investigation and a thermally inert material as a reference compound, as the two materials are heated at a predetermined rate. The TG technique consists of measuring the changes in weight of the sample under investigation, as the sample is heated in a predetermined rate. The DTG technique consists of measuring the rate of weight loss of the samples as it is heated at a specified rate.

The DTA, TG and DTG curves for all the glasses have been taken using "Mom Derivetograph" with a heating rate of 6-7°C/minute, for the glasses numbered 1, 2 and 3. In this instrument the DTA, TG and DTG curves are photographically printed in a continuous manner as a function of temperature. The advantage of this instrument is that all the three types of curves are taken under the identical experimental conditions, since all the three types of curves are taken simultaneously in a single run. Since the informations conveyed by these three techniques are complementary to each other, so in a strict sense they can be compared among themselves only if they are carried out under identical conditions. When it is not possible to resolve the TG peak in thermogravimetric analysis, it is resolvable in the derivative thermogravimetric analysis. Another

advantage of this instrument is that it measures the temperature of the sample. Hence irrespective of heating rate, it always reflects the same temperature at which reaction takes place.

The glasses are ground and the glass particles of size -14 mesh to +20 mesh are sieved out. According to Devies and Kerrison[33] this size is large enough to avoid surface crystallisation. The ground sample of selected size is then mixed with Al_2O_3 powder in the ratio of 70:30 by volume. This prevents the sintering of particles, although the peak height decreases. Sintering is undesirable since it leaves air gaps and also makes the removal of the sample difficult at the end of run.

The exothermic peak observed is due to growth of crystals from glasses. In the expression $\Delta H = \Delta G + T\Delta S$, G is negative in spontaneous process. Since ordering occurs in crystallisation from glasses, ΔS is negative and hence H is negative. This means an exothermic process. The endothermic peak observed is due to nucleation process[33].

3.2.2 Heat Treatment:

The object of heat treatment is to convert the glass sample into a fine grained crystalline material. From the annealed glass rectangular samples are cut with a diamond-tipped cutting wheel. Then the samples are heated in a wire-wound furnace to give the nucleation and growth treatments as determined by the differential thermal analysis. But during heating we have

to be very careful about the heating rate. The importance of heating rate during ceramisation of glasses has been discussed in detail by McMillan[22]. The first stage involves the heating of the sample from room temperature to the nucleation temperature. Here heating rate is not very critical. Heating rate should be such that the thermal stress developed during heating will not lead to cracking of the glass sample. Obviously heating rate is determined by the thickness of the sample and the co-efficient of the thermal expansion of the glass. At the nucleation temperature the samples are held for a period of one hour. The second stage involves the heating of the glass samples from the nucleation temperature to the maximum crystallisation temperature. Here the heating rate is very important. At this stage the heating rate should be sufficiently slow so that crystalline phases will be developed and this in turn will prevent the deformation of the sample at the higher growth temperature. To be on the safe side we have used a heating rate of about 4°C/minute. All the samples are held at their growth temperatures for a period of three hours. Finally the furnace is shut down and the sample is left for furnace cooling. Samples 1S, 1D, 3S, 3D are cooled at the rate of 0.5°C/minute to avoid cracking. The details of the heat treatment and other treatments are listed in Table 3.2.

Table 3.2

Different Treatments Applied to Glasses

Glass No.	Sample No.	Heat Treatment						Ion Exchange in molten $AgNO_3$		Reduction	
		Nucleation		Growth							
		T	t	T	t	T	t	T	t	T	t
1	1S	600	1	750	3	-	-	-	-	-	-
	1D	600	1	750	3	830	3	-	-	-	-
2	2S.1	565	1	630	3	-	-	310	6	320	2.0
	2S.2	565	1	630	3	-	-	310	6	320	1.0
	2S.3	565	1	630	3	-	-	310	6	320	0.5
	2D.1	565	1	630	3	825	3	310	9	320	2.0
	2D.2	565	1	630	3	825	3	310	9	320	1.0
	2D.3	565	1	630	3	825	3	310	9	320	0.5
3	3S	620	1	785	3	-	-	-	-	-	-
	3D	620	1	785	3	925	3	-	-	-	-

T - Temperature in °C.

t - Time in hours.

3.3 ION EXCHANGE TREATMENT

All ceramised glass samples have been subjected to $Na^+ \rightleftharpoons Ag^+$ ion exchange treatment by immersing the samples in molten silver nitrate.

The surfaces of the ceramised samples are ground flat by rubbing with SiC powder of sizes from 120 mesh to 600 mesh. Then the samples are optically polished with 1 micron Al_2O_3 powder, followed by 0.05 Al_2O_3 powder.

The polished glass-ceramic samples are put into the pyrex crucible and the rest of the pyrex crucible is filled with reagent grade $AgNO_3$. The crucible, being kept in a hole of a refractory plate is then introduced in a wire-wound furnace. The temperature is raised to 310°C and $Na^+ \rightleftharpoons Ag^+$ ion exchange takes place in molten $AgNO_3$. After the ion exchange treatment, the sample is taken out of molten $AgNO_3$ and putting the sample on the refractory plate, it is immediately introduced again into the furnace. The furnace is then switched off and the sample is left for furnace cooling. This precaution is taken to avoid cracking due to thermal stresses. The cooled sample is dipped in water for a period of 24 hours to dissolve the traces of silver nitrate adhering to the sample.

3.4 REDUCTION

The ion exchanged samples are kept on a refractory base and introduced in a tube furnace. The hydrogen gas is passed at the rate of 100 cc/minute from the beginning. The temperature is raised slowly to a specified temperature and kept there for a specified period of time. The details of various reduction temperatures and times applied to different ceramised glasses have been given in Table 3.2. After the reduction period is over, the furnace is switched off and when the temperature of the furnace drops down to 100°C, the flow of the hydrogen gas is stopped.

3.5 MEASUREMENT OF BULK ELECTRICAL RESISTIVITY

3.5.1 Resistivity of V,S and D Samples:

The schematic circuit diagram for measuring the DC and AC resistivity dependence on temperature (25°C-350°C) of virgin (V), single heattreated (S) and double heattreated (D) glasses is given in the Fig.3.1. Fig.3.2 gives a schematic view of the resistivity cell fabricated by Kumar[34].

The glasses are cut into pieces (approximately 1x1x0.3 cm^3) and gold is deposited by vacuum evaporation on two opposite surfaces which do not contain the thickness after measuring the actual cross sectional area and thickness of the sample with a micrometer (Mitutoya make). The sample is loaded to the sample holder and the measurements are carried out as follows:

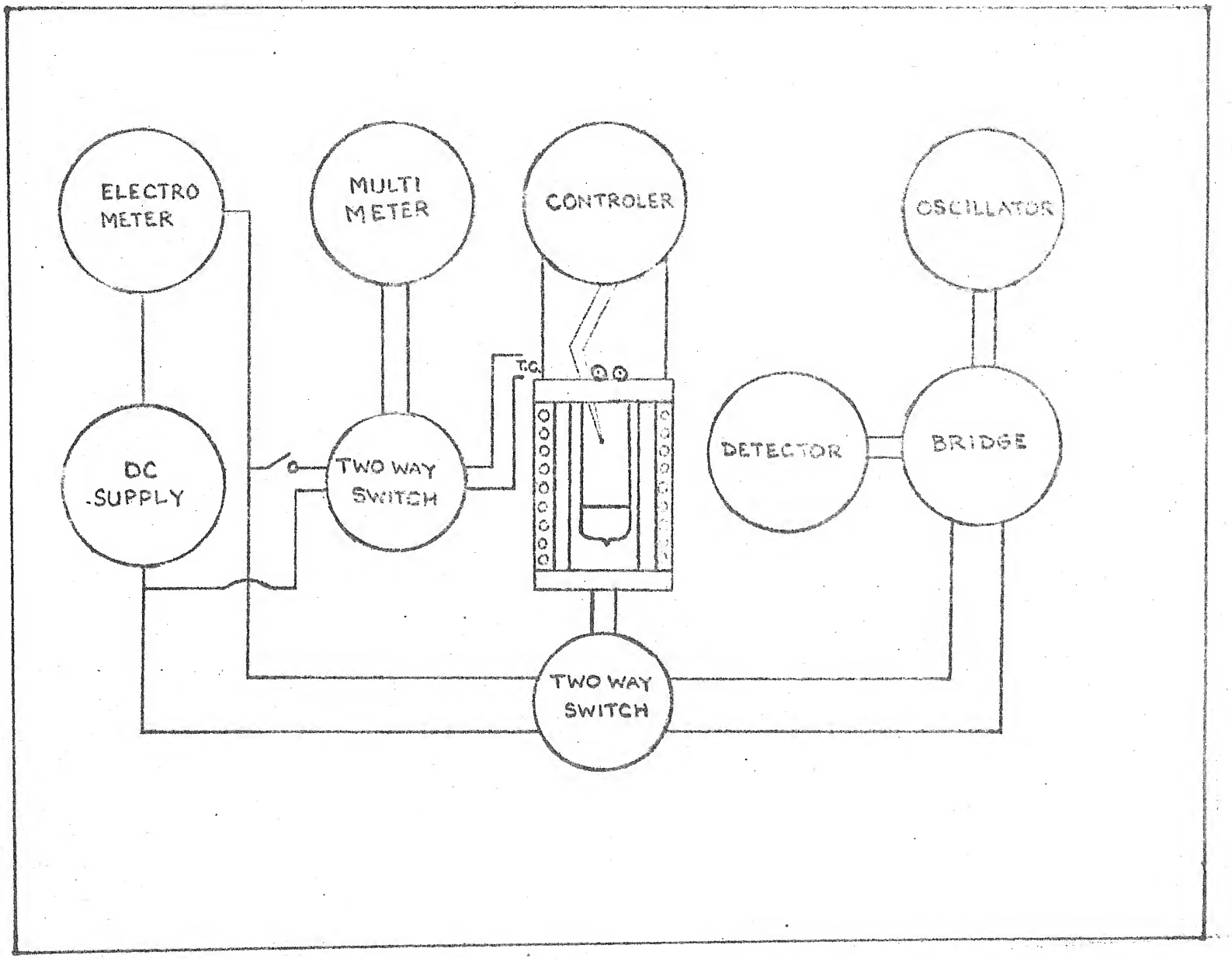
ELECTRO METER
MULTI METER
CONTROLER
OSCILLATOR
T.C.
DC SUPPLY
TWO WAY SWITCH
DETECTOR
BRIDGE
TWO WAY SWITCH

FIG. 3.1

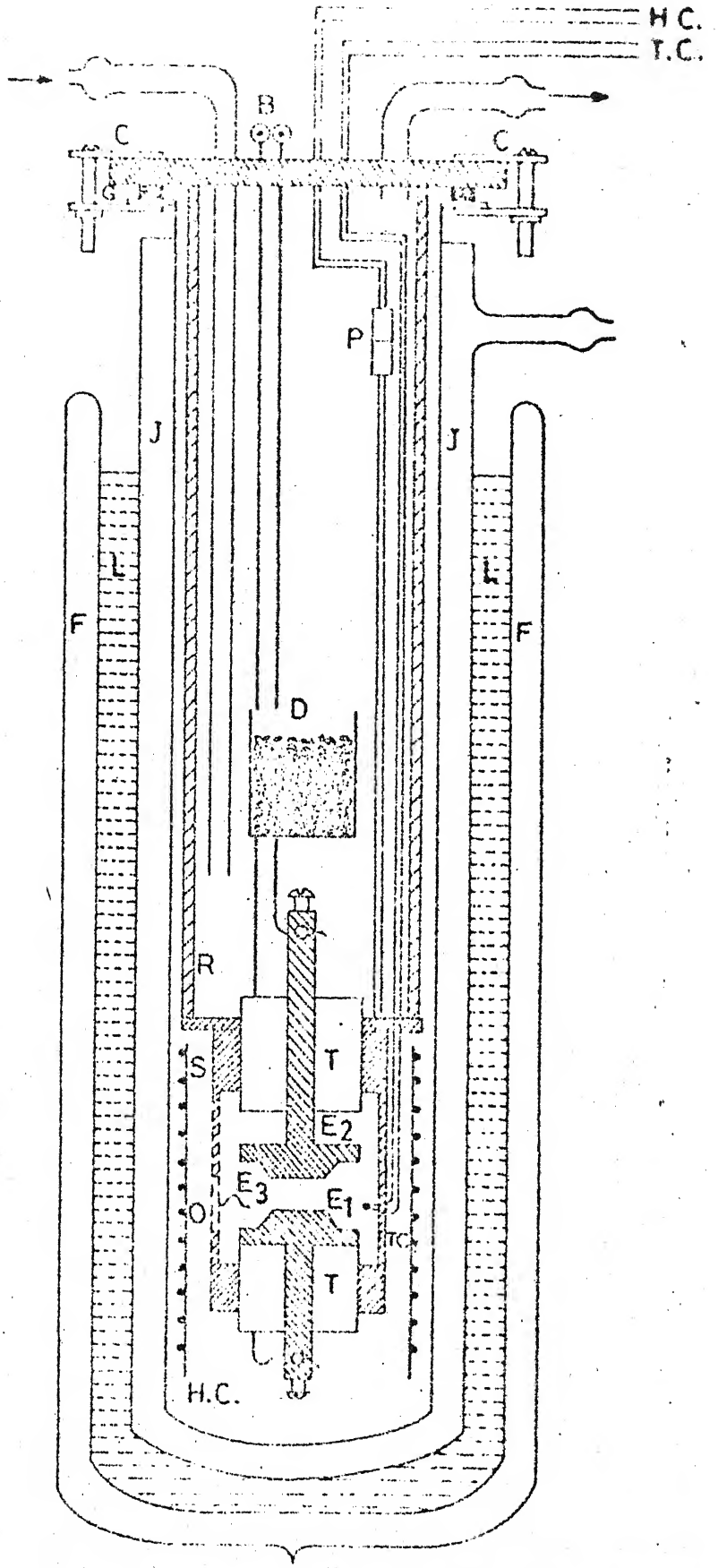

Fig.3.2 Schematic view of the resistivity cell. (Ref 34.)

3.5.1.1. DC Resistivity:

At different temperatures in the region of 25°C-350°C the current through the sample (I amp.) is measured with an electrometer (610C solid state, Keithley Instruments) for a certain voltage (V). This is done for applying different voltages (0-10 V). The slope of the I-V plot is the resistance (R Ohm.) of the sample at that temperature. The DC resistivity at that temperature is given by

$$\rho_{DC} = R \frac{A}{t} \qquad (3.1)$$

where ρ_{DC} the resistivity in ohm-cm, A the area of cross section in cm^2, t the thickness in cm.

3.5.1.2 AC Resistivity:

In the temperature region of 25°C-300°C the AC resistivity of the samples are measured by bridge balance method using transformer ratio arm capacitance bridge (GR 1615-A) with an oscillator (GR1210C) tuned amplifier and null detector (GR1232A) measuring the capacitance C and dissipation factor D of the samples. The AC resistivity ρ_{AC} is given by

$$\rho_{AC} = A \frac{1}{2\pi f t C D} \qquad (3.2)$$

where A is the area of cross section in cm^2, t thickness in cm, f is the frequency of applied field in Hz. The $_{AC}$ at each temperature was measured for frequencies 0.1, 0.2, 0.5, 1.0, 2.0, 5.0, 10.0, 20.0, 50.0, 100.0 KHz.

3.5.2 DC Resistivity of Ion Exchanged and Reduced Samples:

The schematic circuit diagram for measuring the DC resistivity of ion exchanged and reduced samples is given in the Fig.3.3. The same resistivity cell is used as before Fig.3.2 . All the four surfaces which do not contain the length and thickness of the sample are removed to avoid parallel path and on the two surfaces which do not contain the length, gold is deposited by vacuum deposition after measuring the length and thickness of the sample by the micrometer. The sample is loaded to the sample holder and the measurement is carried out as follows.

At different temperatures in the region of room temperature to 25°C less than the reduction temperature the current-voltage characteristic is studied. The slope of the I-V plot is the resistance R (ohm) at that temperature. The bulk resistivity of the conducting layer is given by:

$$\rho_c = 2 \times R \frac{A}{t}$$

∴ Temperature coefficient of resistance

$$TCR = \frac{1}{\rho_{c_{RT}}} \frac{d\rho_c}{dT} \qquad (3.3)$$

where $\rho_{c_{RT}}$ is the resistivity at room temperature and $\frac{d\rho_c}{dT}$ is the slope of ρ_c -T plot.

The resistivity during cooling is also noted and it is found that the resistivity has decreased. The sample is

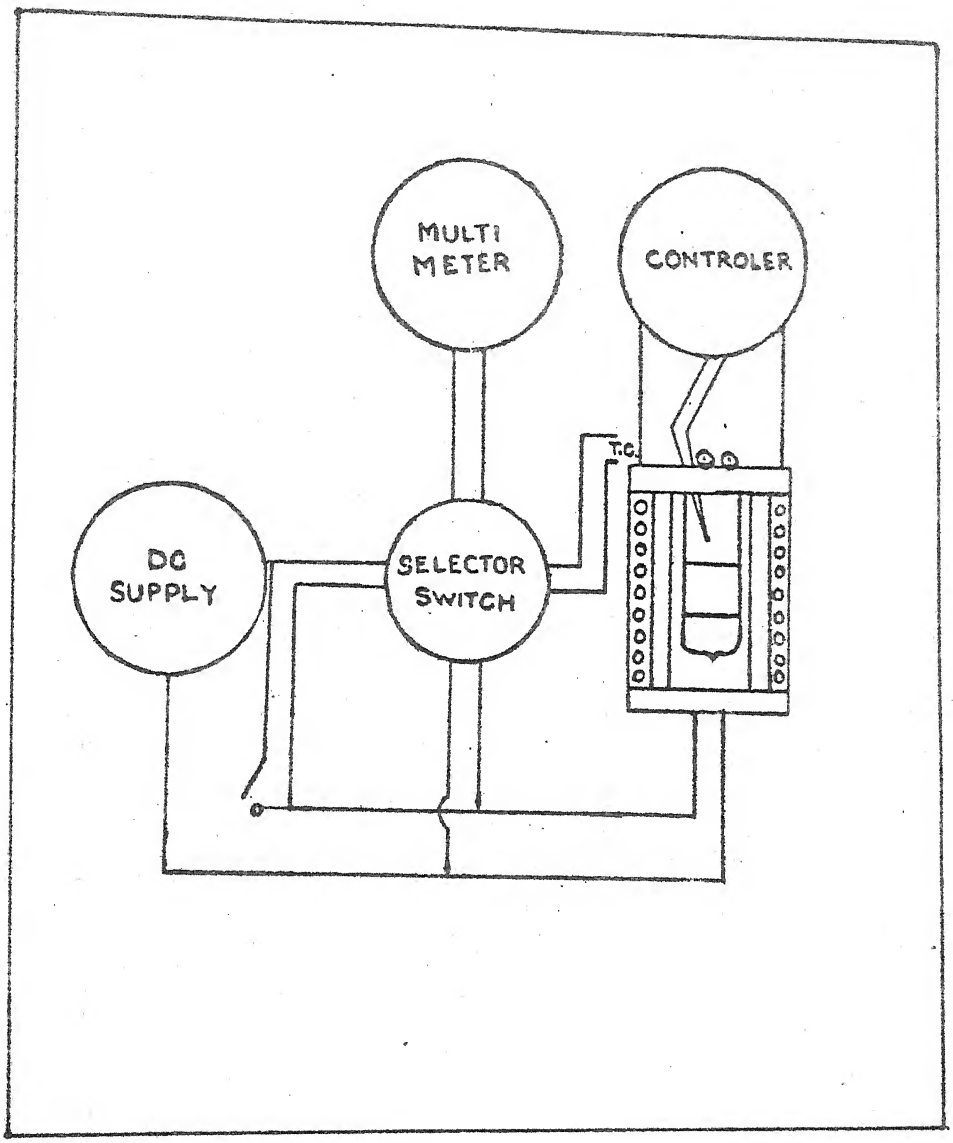

FIG. 3·3

heated again and the resistivity is measured during heating and cooling. This cycle is repeated till a stable resistivity is obtained which remains same during heating and cooling.

3.6 DETERMINATION OF THICKNESS OF CONDUCTING LAYERS

The thickness of the conducting layers is determined by taking the scanning electron micrographs in a ISI 60 Scanning Electron Microscope. The cross checking is done by measuring the surface resistance as a function of the thickness of the conducting layers[10]. The thickness measured by both methods are found to be almost same.

3.7 MICROSCOPIC STUDY

3.7.1 Sample Preparation and Photographic Printing of Microstructure:

In the usual way as discussed in the preparation of the sample for ion exchange, some of the samples are optically polished to 0.05 μ. Gold is deposited by vacuum evaporation on the polished surface and the scanning electron micrograph is taken in a ISI 60 Scanning Electron Microscope.

3.7.2 Determination of Percent Volume Crystallisation:

Assuming the crystallisation is homogeneous throughout the bulk of the material, we can use the point counting method to find the % volume crystallisation by the following expression

$$\text{Volume crystallisation} = \left(\frac{n}{N} \times 100\right)\% \qquad (3.4)$$

where,

n = number of points coinciding with the crystalline phases

N = total number of points present in the selected area of the transparent graph paper.

Making use of the above expression we have calculated the % volume crystallisation for different ceramised glasses.

3.8 X-RAY DIFFRACTION STUDY

X-ray diffraction study has been carried out to identify the crystalline phases present in the ceramised glasses. All the glass compositions have been ceramised as in Table 3.2. Particle sizes used for taking the diffraction pattern by X-ray diffractometer are below 325 mesh.

The fundamental law in X-ray diffraction is the Bragg law and is given by the expression,

$$2d \sin\theta = n\lambda \qquad (3.5)$$

where d is the interplanar spacing, θ is the Bragg angle and λ is the monochromatic radiation used for the diffraction purpose. From the above expression we can calculate the interplanar spacings for different Bragg angles. The interplanar spacings are characteristics of a particular crystal structure and they are associated with particular relative intensities, for a particular crystalline material. Hence by comparing these d values with the

standard data such as A.S.T.M. Index and also by matching the relative intensity data, one can identify the unknown crystalline materials.

In X-ray diffractometry we get a continuous plot of relative intensity versus 2θ, where θ is the Bragg angle. Hence from these relative intensity versus 2θ graphs we will get the necessary data to carry out the identification of the crystals developed during ceramisation of the glasses.

3.9 TRANSMISSION ELECTRON MICROSCOPIC (TEM.) STUDY

TEM analysis is carried out for virgin glass samples. The TEM samples are prepared by the conventional method of preparing glass samples for TEM study[14]. The transmission electron microstructure of the samples at 100 kV are taken in a Phillips EM 301 Transmission Electron Microscope.

CHAPTER 4

RESULTS

4.1 THERMAL ANALYSIS

The thermal analysis curves for the glass samples 1, 2 and 3 have been shown respectively in figures 4.1, 4.2 and 4.3. The nucleation and growth temperatures for all the glasses as obtained from the corresponding DTA curves have been written on the respective figures. The endothermic and exothermic peaks have been attributed to nucleation and growth respectively, because of the reasons explained earlier in Chapter 3.

4.2 X-RAY DIFFRACTION STUDIES

The relative intensity versus 2θ curves for all ceramised glasses, obtained by X-ray diffraction are shown in Figures 4.4.1S, 4.5.1D, 4.6.2S, 4.7.2D, 4.8.3S and 4.9.3D. The last number in figures represent the glass number as mentioned in Table 3.2.

For d-spacings calculation we have made use of computer. The computer program is given in Appendix 2. From the calculated d-values and the corresponding relative intensity values, identification of unknown crystalline phases are done comparing with the standard data from A.S.T.M. index. All the X-ray diffraction data for 1S, 1D, 2S, 2D, 3S, 3D samples are given in Tables 4.1, 4.2, 4.3, 4.4, 4.5 and 4.6 respectively.

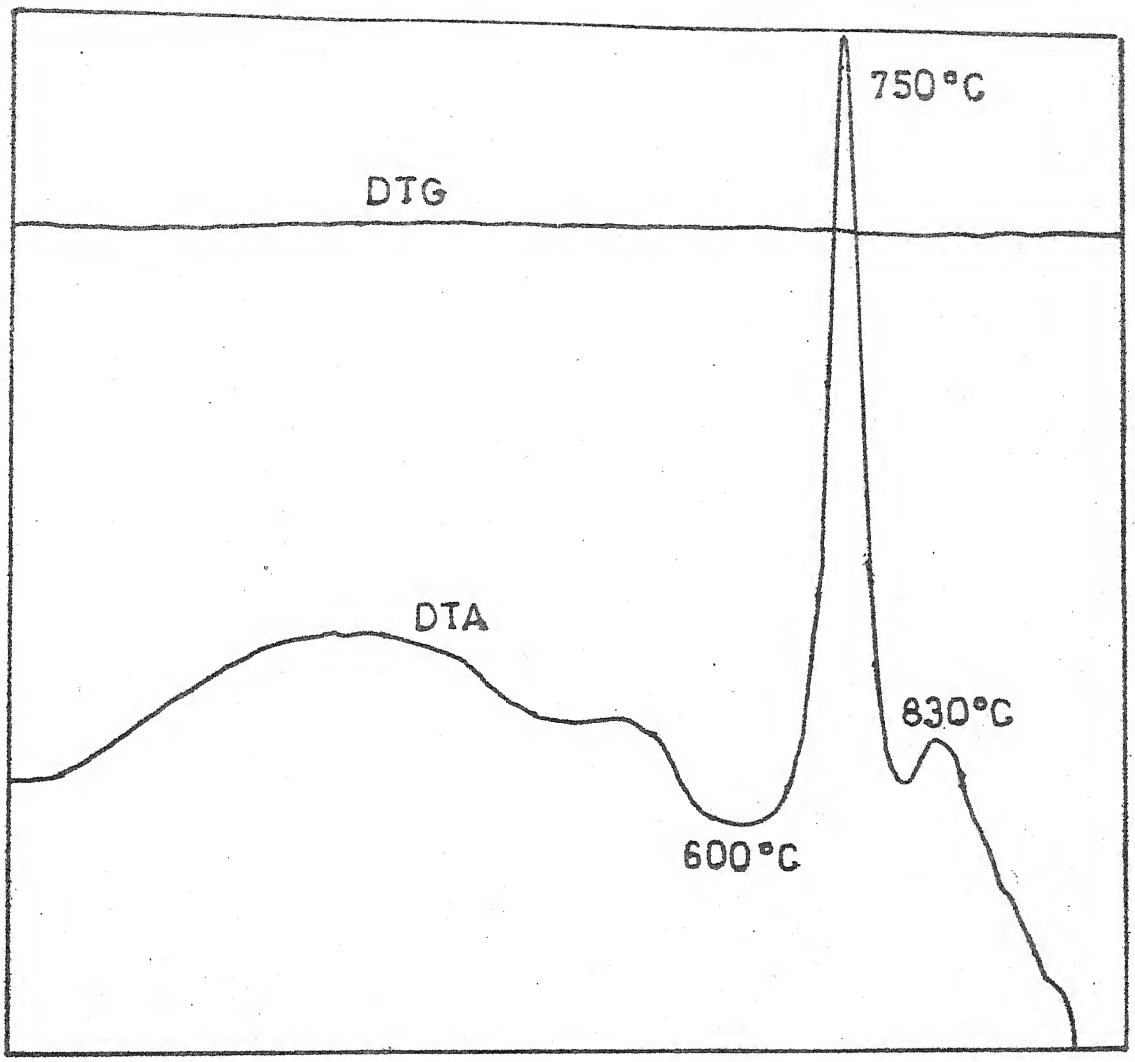

FIG. 4-1

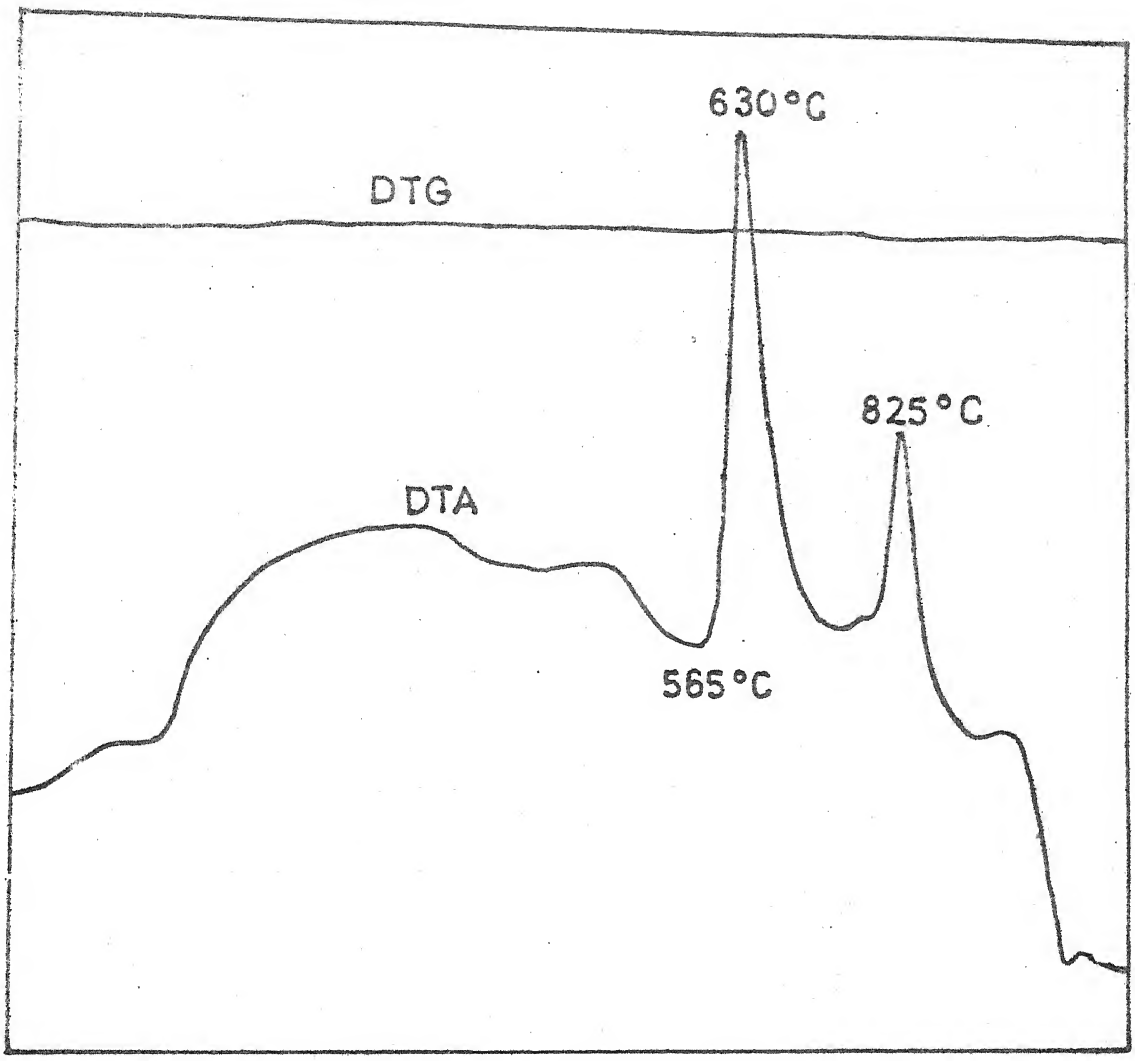

FIG. 4-2

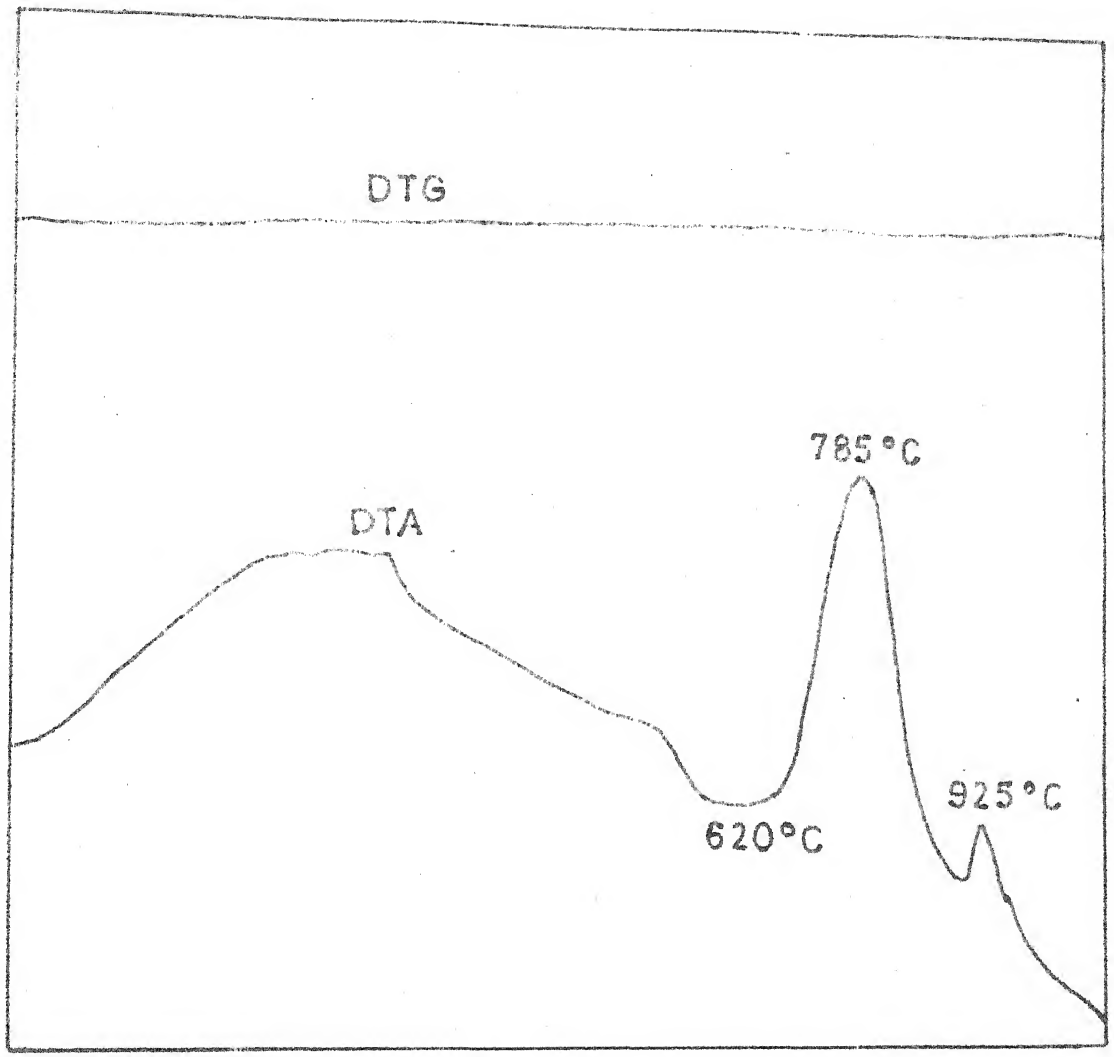

FIG. 4-3

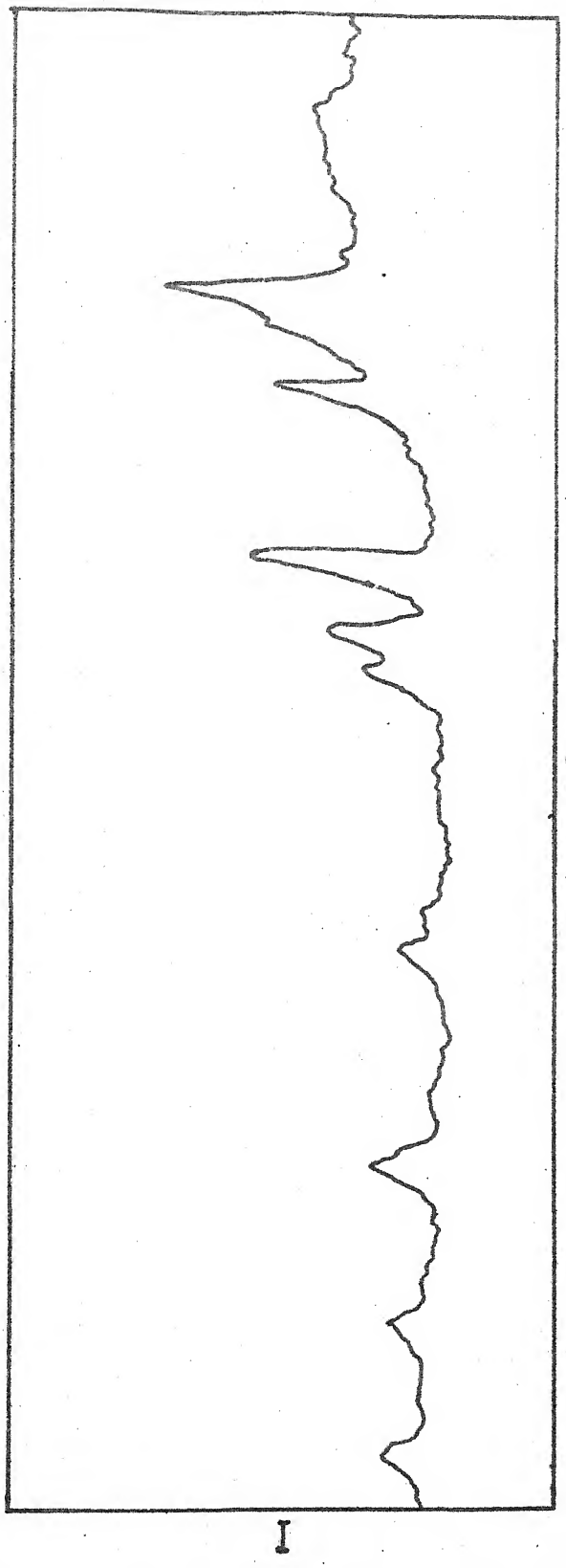

FIG. 4.4.1 S

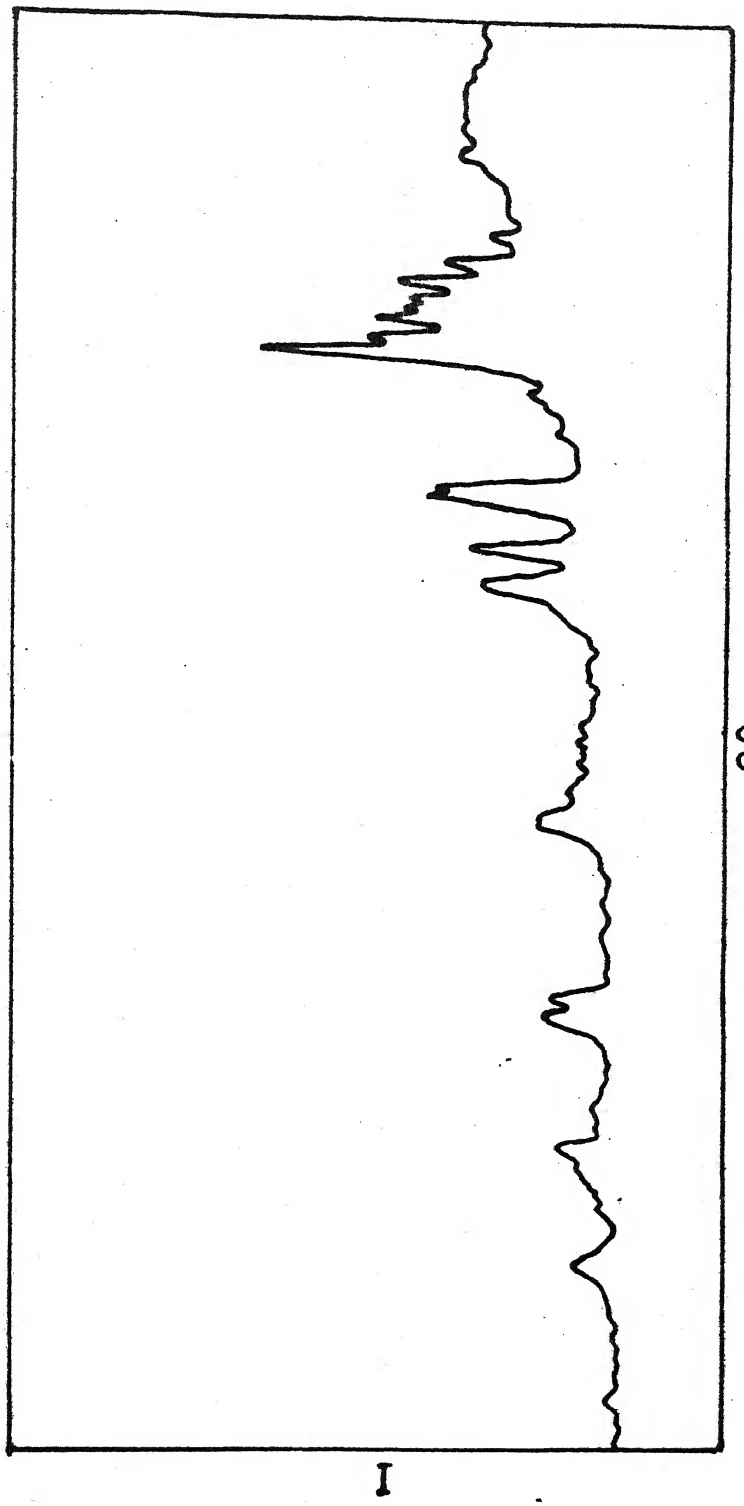

FIG. 4.5.1D

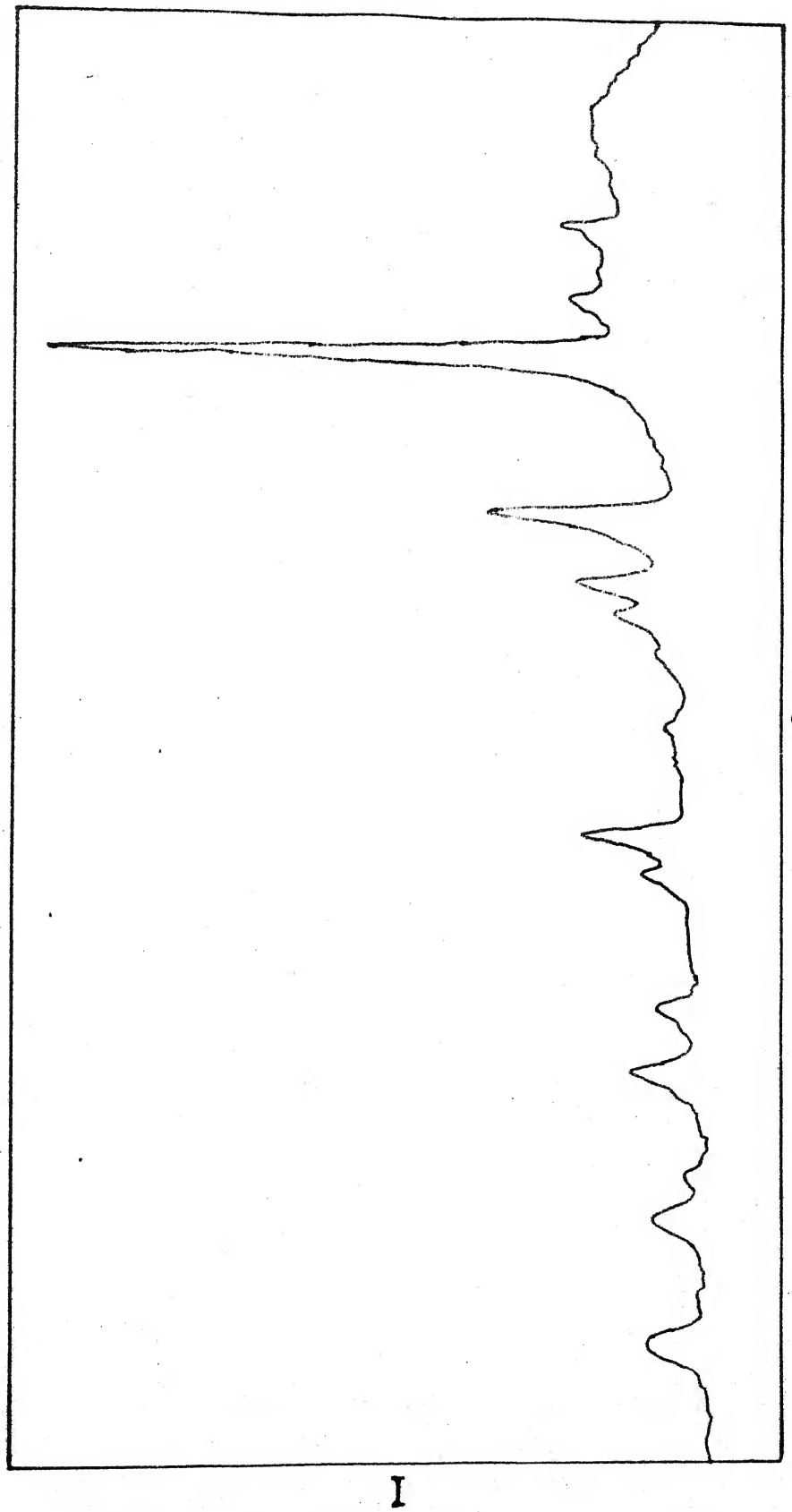

FIG. 4.6.2S

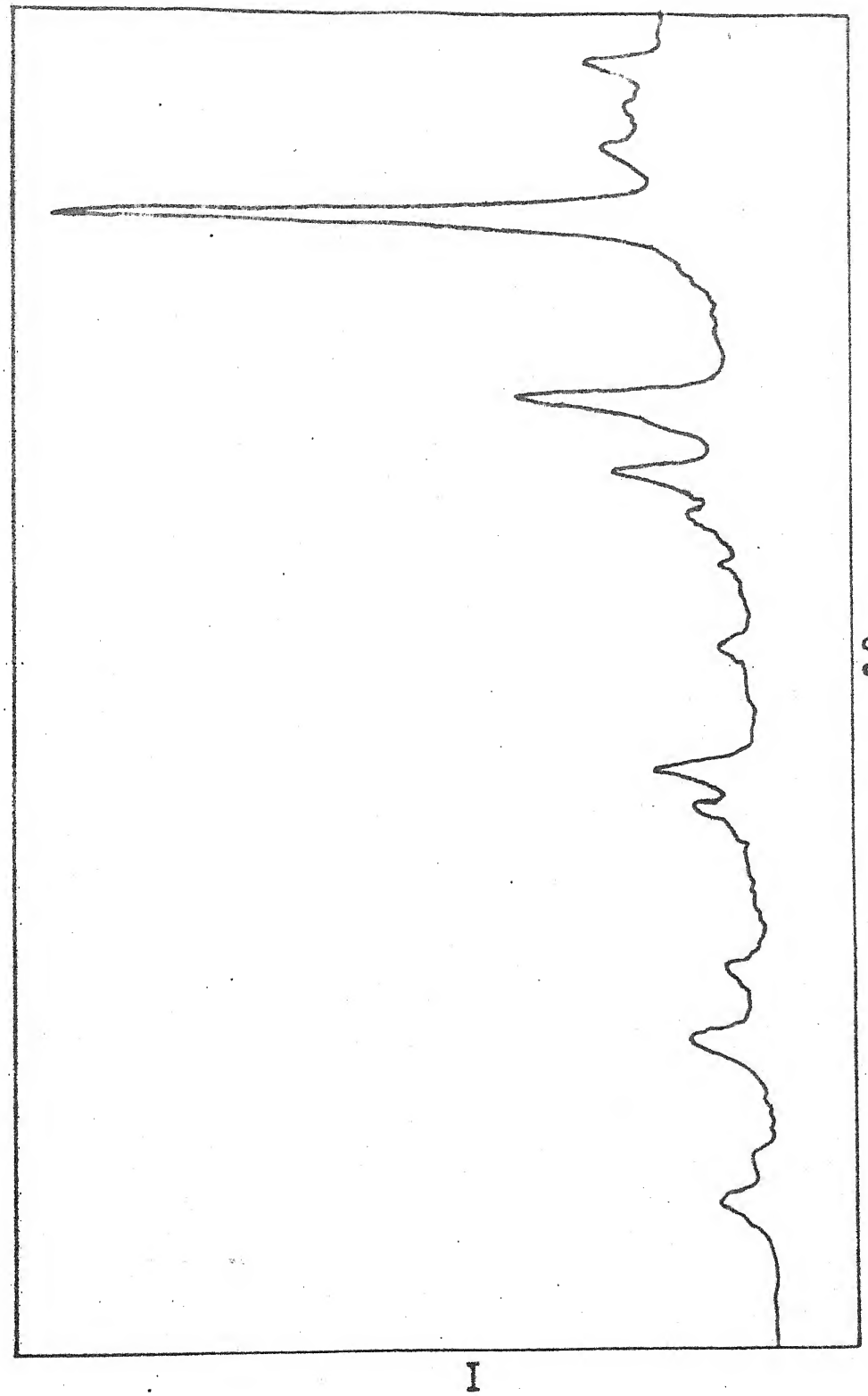

FIG.4.7.2D

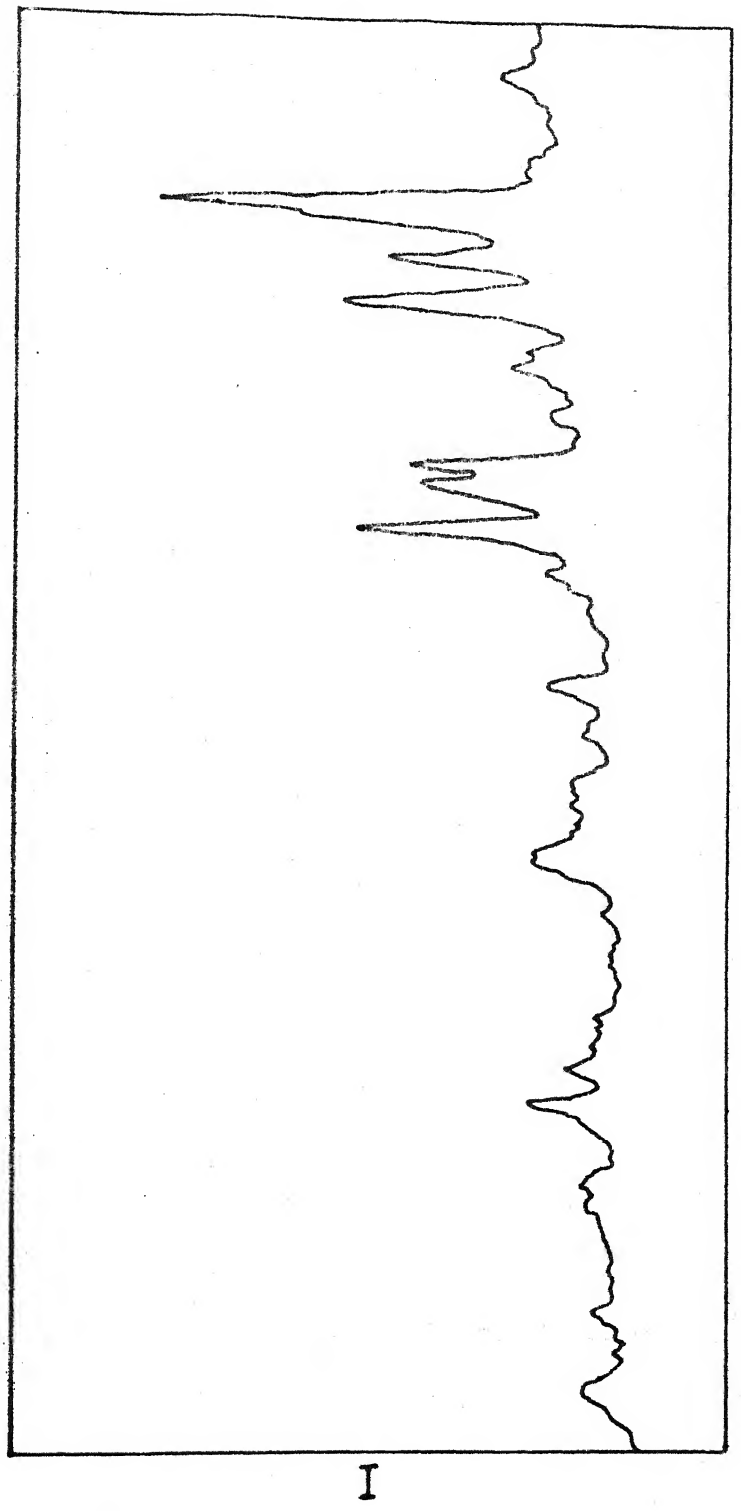

FIG. 4.8.3S

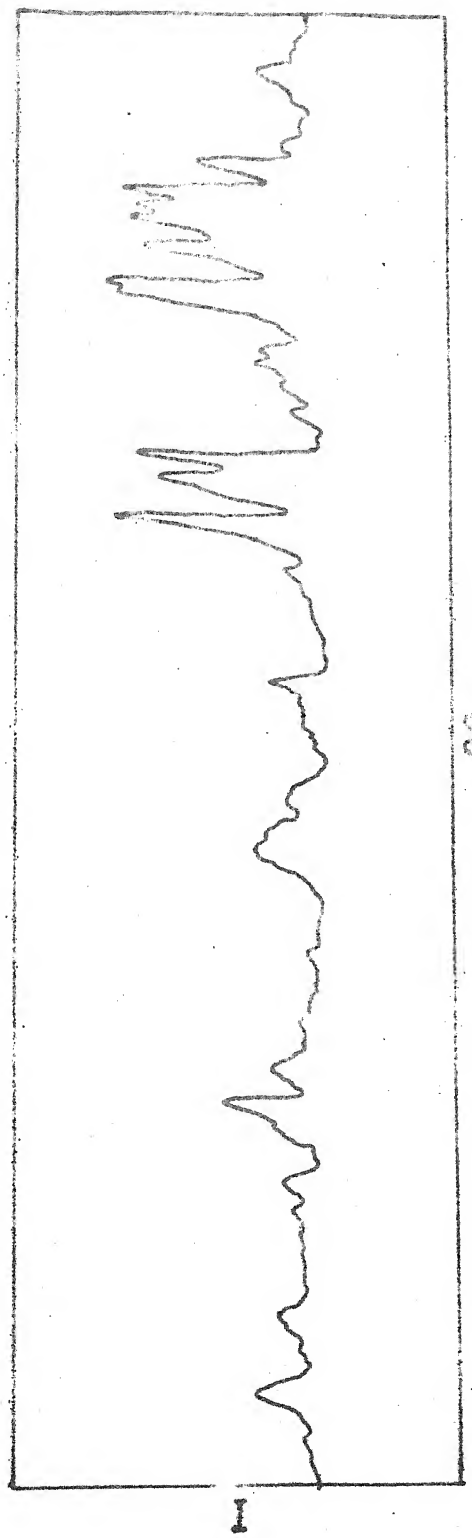

FIG. 4·9·3D

		[illegible] PHOSPHATE	
[illegible]	[illegible]	ER SPACING ÅNGSTRÖM	RELATIVE INTENSITY
[illegible]	[illegible]	2301	35.0
[illegible]	[illegible]	9741	100.0
[illegible]	[illegible]	8902	100.0
[illegible]	[illegible]	5571	55.0
[illegible]	[illegible]	3676	25.0
[illegible]	[illegible]	3422	65.0
[illegible]	[illegible]	3162	35.0
[illegible]	[illegible]	2250	30.0
[illegible]	[illegible]	2049	2.0
[illegible]	[illegible]	1583	4.0
[illegible]	[illegible]	1717	4.0
[illegible]	[illegible]	1006	2.0
[illegible]	[illegible]	0805	2.0
[illegible]	[illegible]	0405	4.0
[illegible]	[illegible]	7855	14.0
[illegible]	[illegible]	7705	10.0
[illegible]	[illegible]	7088	2.0
[illegible]	[illegible]	6791	2.0
[illegible]	[illegible]	6429	2.0
[illegible]	[illegible]	6097	4.0
[illegible]	[illegible]	5300	12.0
[illegible]	[illegible]	5165	16.0
[illegible]	[illegible]	3788	14.0
[illegible]	[illegible]	0000	0.0
[illegible]	[illegible]	0000	0.0
[illegible]	[illegible]	0000	0.0
[illegible]	[illegible]	0000	0.0

From Table 4.1 we observe that the data for the crystalline phase in this ceramised glass, match reasonably with those for zinc slicate. Hence the crystalline phase developed in sample No.1S is concluded to be zinc silicate. However a few weaker peaks are present which do not coincide with those of the phases mentioned. So there will be some other silicates of minor amount.

From Table 4.2 we observe that the data for the crystalline phases in this glass, match reasonably well with those of lithium phosphate. The presence of zinc silicate is also there along with some other minor silicates.

From Table 4.3 we can conclude that lithium phosphate phase is there in this glass along with some other minor silicates.

In Table 4.4 we see that there is no change with Table 4.3. So no phase other than phosphatesilicate along with some other minor silicates is present there.

From Table 4.5 we observe that the data for the crystalline phase in this ceramised glass, match reasonably well with those for zinc silicate. Hence the crystalline phase developed in sample No.3S is concluded to be zinc silicate. However a few weaker peaks are present which do not coincide with those of the phase mentioned. So there will be someother silicates of minor amount.

From Table 4.6 we observe that the data for the crystalline phases in this glass, match reasonably well with those

of lithium phosphate. The presence of zinc silicate is also there along with some other minor silicates.

4.3 RESISTIVITY OF VSD SAMPLES

4.3.1 DC Resistivity-Temperature

All the data are plotted and given in Figures 4.11, 4.12 and 4.13. The I-V plot are found to be linear in all cases. A representation plot is given in Figure 4.14. The resistances are calculated by finding the slope of the I-V plot by least square method. The resistivity is calculated using equation (3.1) and the computer program used for it is given in Appendix 3. The activation energy is calculated by using the Arrhenius equation

$$\rho = \rho_0 \exp (E/kT)$$

where,

ρ = resistivity in ohm-cm

ρ_0 = pre-exponential factor

E = activation energy in eV

k = Boltzmann constant

T = absolute temperature in °K.

The activation energy for different samples are given in Table 4.7.

4.3.2 AC Resistivity-Temperature

The representative AC resistivity-temperature data are given in Table 4.8, 4.9, 4.10, 4.11 and 4.12. One

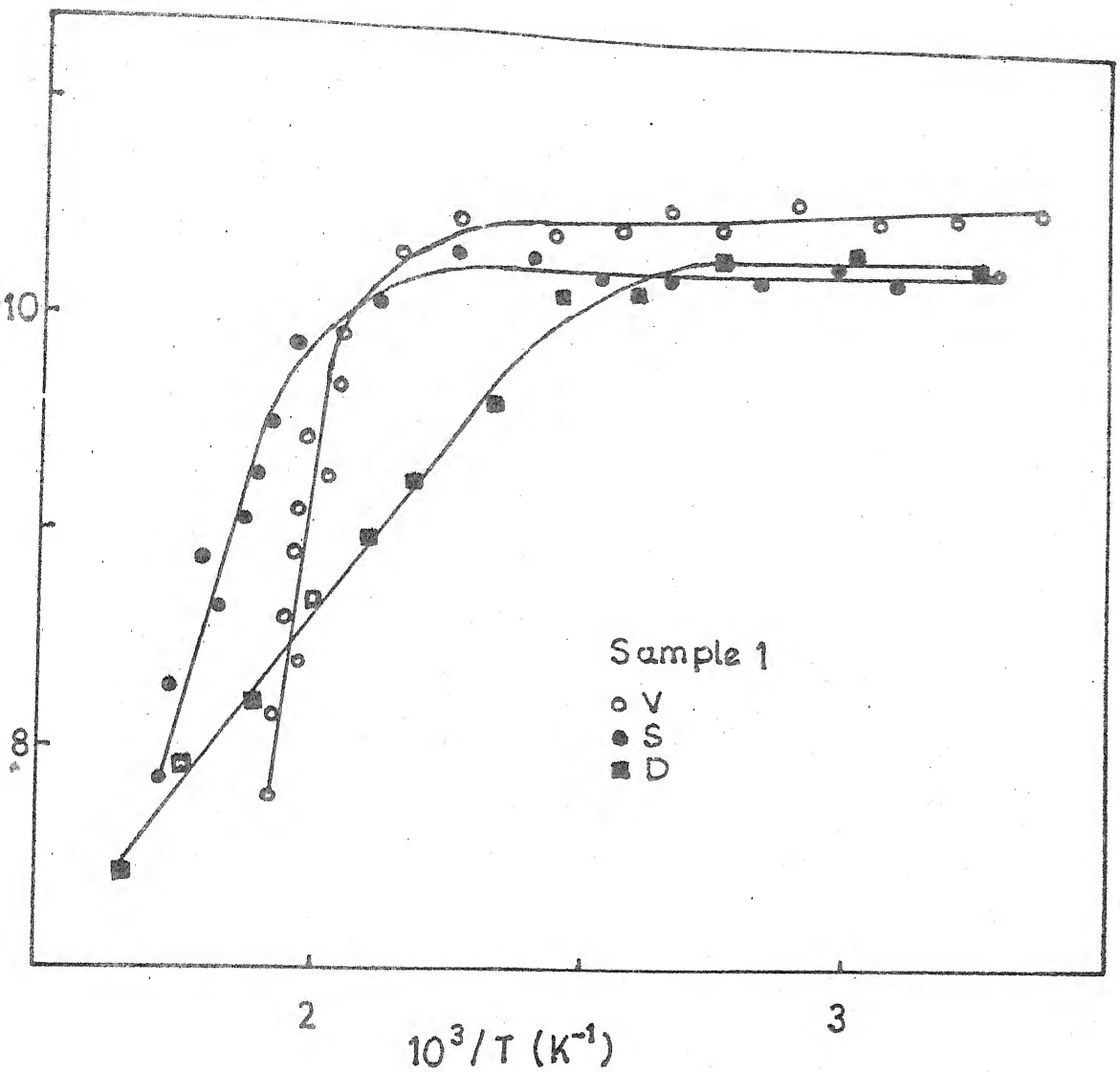

FIG. 4-11

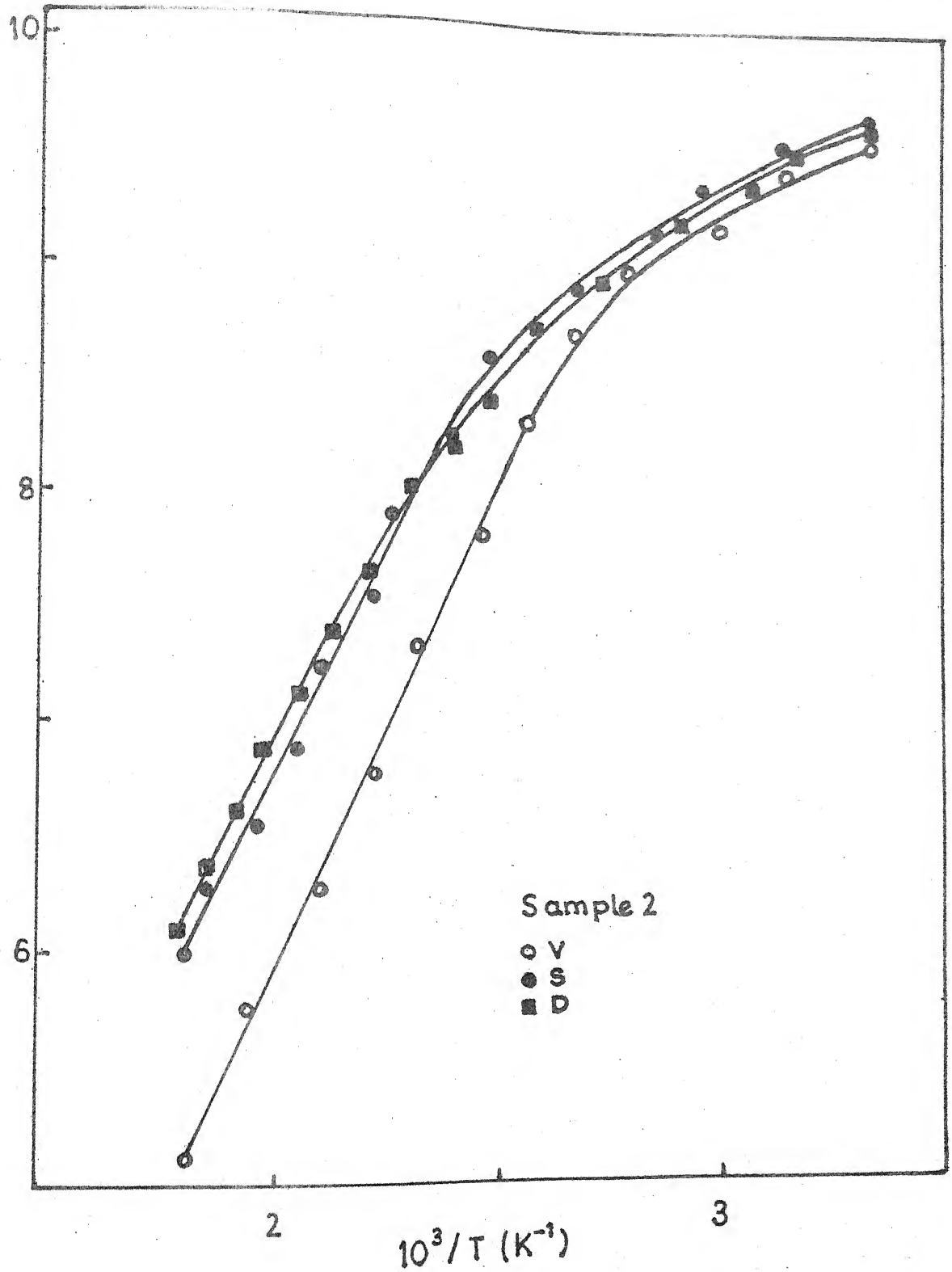

FIG. 4.12

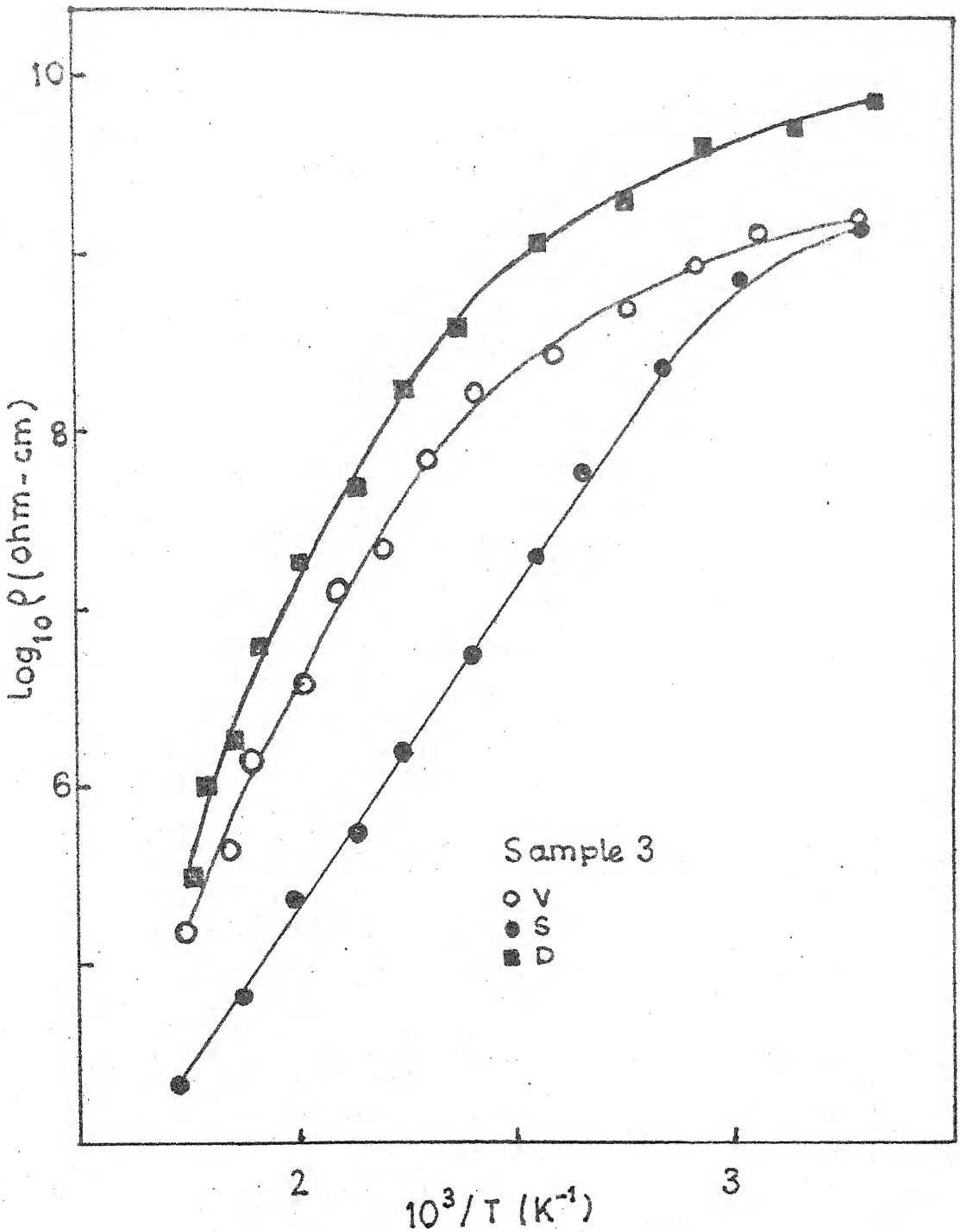

FIG. 4·1 3

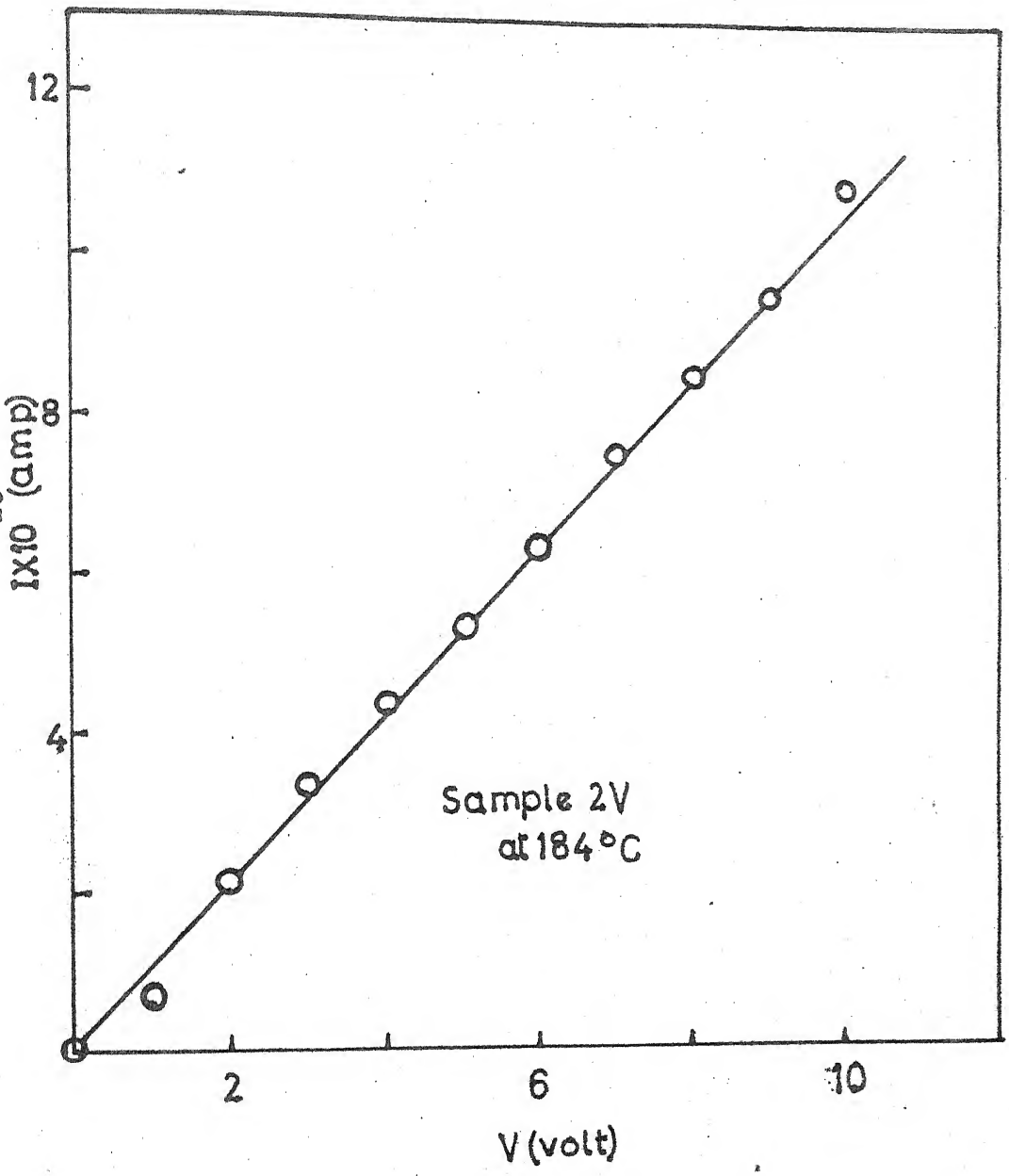

FIG.4.14

TABLE 4.7

Activation Energy of Different Glasses

Sample	Temperature °C	E in eV
1V	25	0.03
	300	3.86
1S	25	0.01
	300	1.90
1D	25	0.008
	300	0.67
2V	25	0.22
	300	0.84
2S	25	0.23
	300	0.81
2D	25	0.24
	300	0.75
3V	25	0.18
	300	0.91
3S	25	0.08
	300	0.80
3D	25	0.18
	300	0.95

Temperature - AC Resistivity Data for 3S

Temperature °C	LOG RESISTIVITY (Ohm-cm) AT FREQUENCIES (KHZ)									
	.1	.2	.5	1.0	2.0	5.0	10.0	20.0	50.0	100.0
31	6.7730	6.6148	6.4345	6.2262	6.0334	5.7238	5.4627	5.1816	4.8119	4.5176
92	6.8906	6.6115	6.4893	6.2695	6.0645	5.7411	5.4656	5.1830	4.8062	4.5119
147	6.5047	6.4566	6.2652	6.1094	5.9385	5.6530	5.4049	5.1355	4.7718	4.4826
196	-	5.6924	5.6191	5.5698	5.5105	5.3696	5.2073	5.0014	4.6998	4.4208
260	-	-	-	4.5639	4.5987	4.6031	4.5521	4.4843	4.3585	4.2072
309	-	-	-	-	4.1089	4.0644	4.0384	3.5749	3.9758	3.9148

Temperature-AC Resistivity Data for 3D

Temperature °C	LOG RESISTIVITY (Ohm-cm) AT FREQUENCIES (KHZ)									
	.1	.2	.5	1.0	2.0	5.0	10.0	20.0	50.0	100.0
28	7.6974	7.5334	7.4291	7.1567	6.9266	6.5909	6.3109	6.0232	5.6424	5.3388
115	7.8598	7.6085	7.3723	7.1529	6.9160	6.5885	6.3111	6.0222	5.6426	5.3518
152	7.6834	7.5629	7.2961	7.0877	6.8710	6.5647	6.2929	6.0088	5.6373	5.3274
193	7.2563	7.1373	7.0232	6.8652	6.7049	6.4486	6.2114	5.9514	5.6005	5.3089
269	-	6.4475	6.0255	5.9982	5.9568	5.8648	5.7463	5.6026	5.3009	5.1518

TABLE 4.10

Temperature - AC Resistivity Data for 1V

Temperature °C	LOG RESISTIVITY (Ohm-cm) AT FREQUENCIES (KHZ)									
	.1	.2	.5	1.0	2.0	5.0	10.0	20.0	50.0	100.0
25	7.5658	7.4272	7.1729	6.9240	6.6744	6.3200	6.0433	5.7691	5.4126	5.1062
118	7.6560	7.4718	7.1294	6.9050	6.6779	6.3566	6.0799	3.7801	5.3717	5.0301
172	7.5978	7.4569	7.1679	6.9657	6.7630	6.3434	6.0478	5.7574	5.3943	5.0940
216	7.5793	7.2799	7.1555	6.9240	6.7025	6.1496	6.0839	5.7899	5.3909	5.0767
249	-	-	-	5.8792	5.7858	-	5.0434	4.8832	4.0766	4.8726
305	-	-	-	-	-	4.1775	4.3075	4.2625	4.2455	4.2000

Temperature - AC Resistivity Data for 1S

Temperature °C	LOG RESISTIVITY (Ohm-cm) AT FREQUENCIES (KHZ)									
	.1	.2	.5	1.0	2.0	5.0	10.0	20.0	50.0	100.0
32	7.6426	7.5242	7.2524	7.0292	6.7968	6.4639	5.8566	5.8913	5.5340	5.2475
104	7.7396	7.5242	7.2667	7.0658	6.8301	6.5144	6.2387	5.9401	5.5336	5.1998
144	7.7064	7.4078	7.2835	7.0622	6.8435	6.5215	6.2489	5.9605	5.5700	5.2468
231	7.6583	7.5457	7.2176	6.9964	6.7697	6.4717	6.2117	5.9344	5.5564	5.2533
305	7.0488	6.6061	6.4907	6.3773	6.2757	6.1159	5.9503	5.7527	5.4673	5.2212

TABLE 4.12

Temperature - AC Resistivity Data for 1D

Temperature °C	LOG RESISTIVITY (Ohm-cm) AT FREQUENCIES (KHZ)									
	.1	.2	.5	1.0	2.0	5.0	10.0	20.0	50.0	100.0
28	7.5158	7.3048	7.0287	6.7866	5.5487	6.1701	5.8372	5.5035	5.1186	4.8409
135	7.5255	7.3611	7.0148	6.8124	6.5684	6.2331	5.9536	5.6527	5.2429	4.8910
189	7.2816	7.1222	6.8924	6.7012	4.6872	6.1795	5.9116	5.6320	5.2513	4.9364
256	6.7712	6.6916	6.5817	6.4536	6.3002	6.0526	5.8210	5.5670	5.2179	4.9203
334	6.7381	5.2060	6.1006	6.0383	5.9636	5.8076	5.6456	5.5055	5.1713	4.8937

representative plot is given in fig.4.15. The log resistivity values are plotted against log frequencies. It is found that it follows $\rho \propto f^{-s}$ relationship, s is calculated from the slope of the straight line. All the s values are given in Table 4.13. One representative log ρ vs log f (Hz) is given in Fig.4.16.

4.3.3 Thickness of the Conducting Layer:

The scanning electron micrographs are given in figures 4.17, 4.18, 4.19, 4.20, 4.21 and 4.22. The thickness of the conducting layer is tabulated in Table 4.14.

4.3.4 Resistivity Values of Ion Exchanged Glasses:

The resistivity versus temperature data are plotted in figures 4.23, 4.24, 4.25, 4.26, 4.27 and 4.28. The slope is calculated by using least square method and the TCR values are calculated by using equation 3.3 and the computer program is given in Appendix 4.

4.4 SCANNING ELECTRON MICROGRAPH

The micrographs are given in figures 4.29, 4.30, 4.31, 4.32, 4.33 and 4.34 for the samples 1S, 1D, 2S, 3S, 3D respectively using equation 3.4 we have calculated the volume crystallisation. The microstructural data are summarised in the Table 4.15.

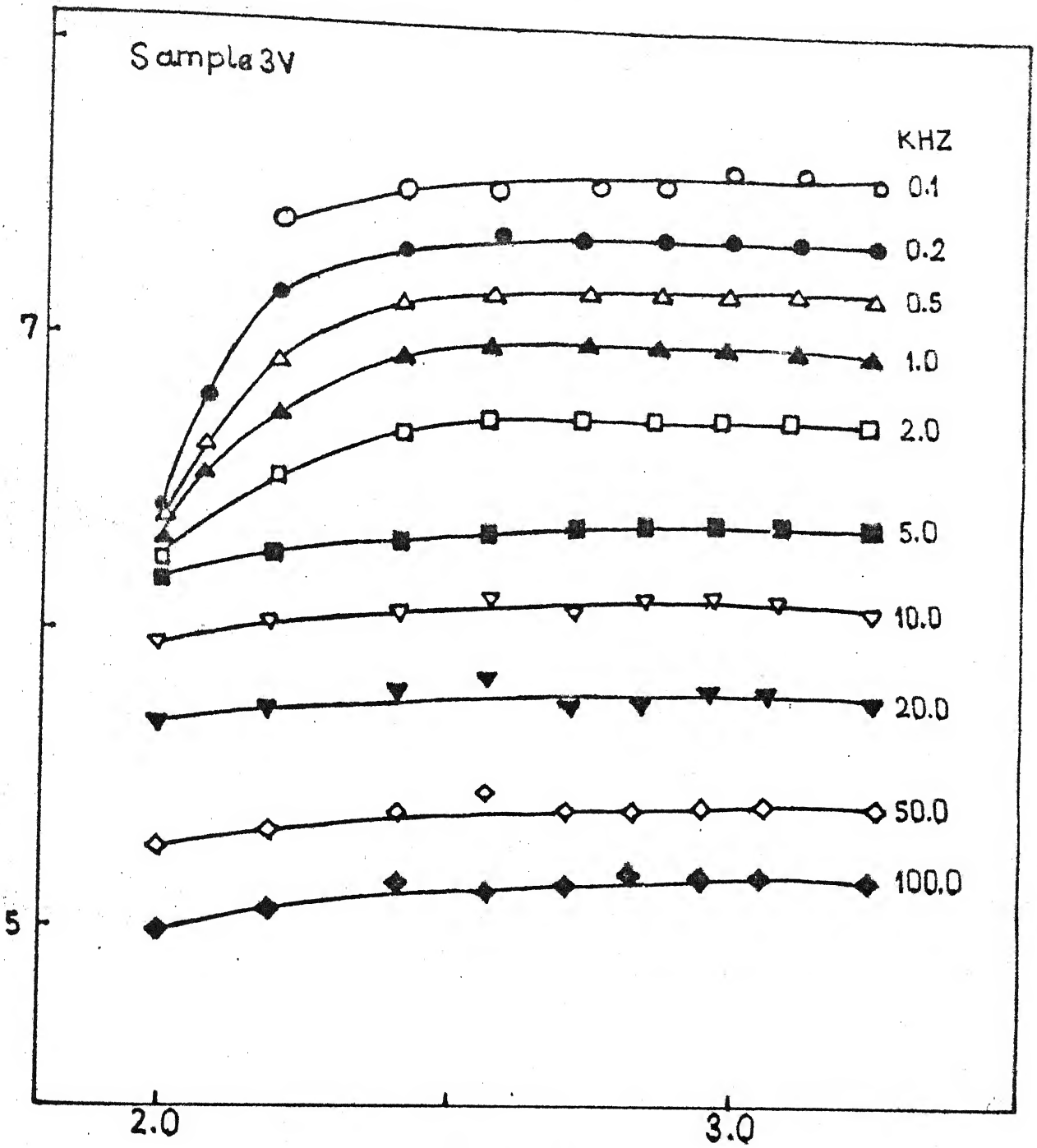

FIG. 4.15

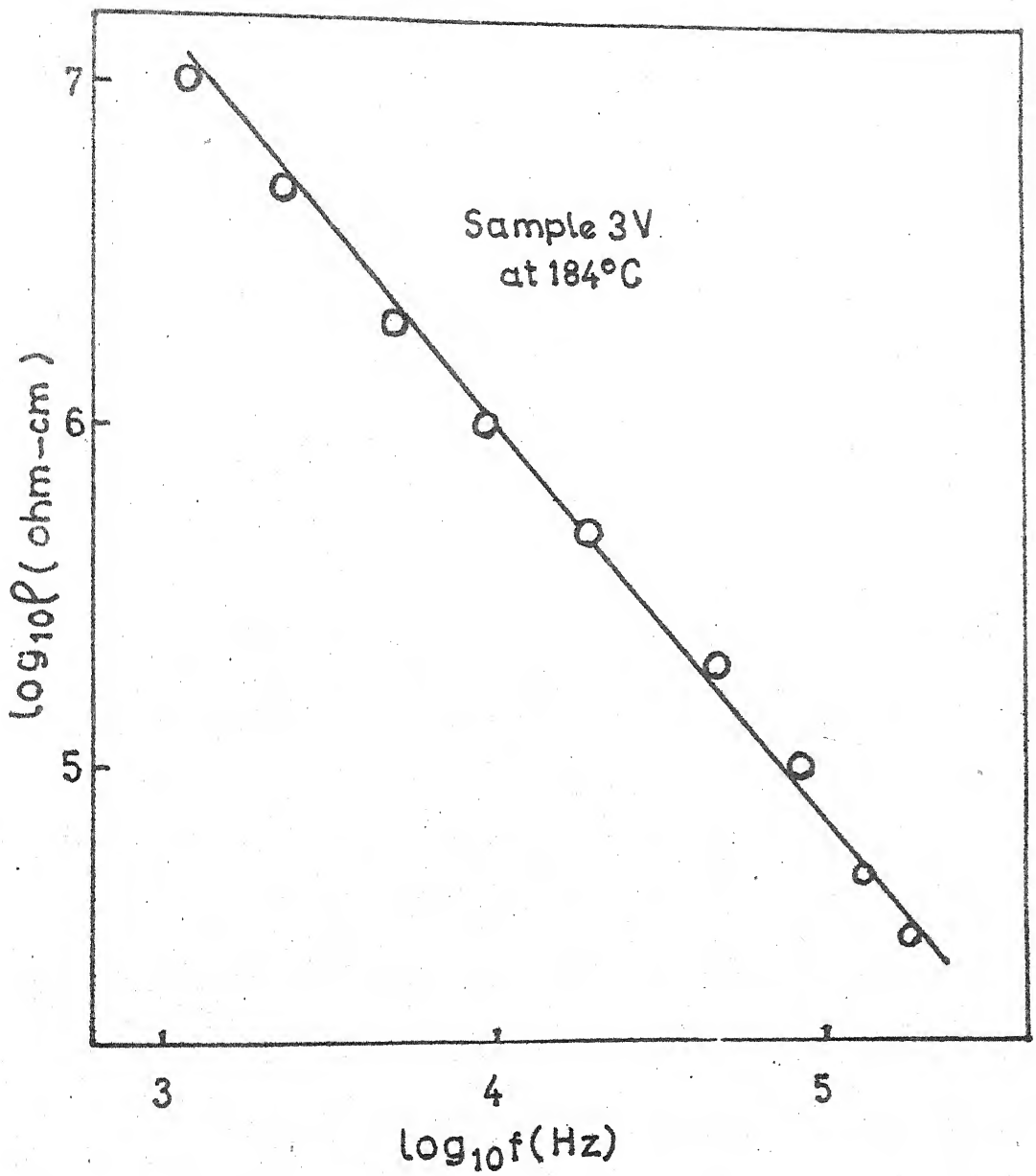

FIG. 4-16

TABLE 4.13

s Values of Samples

Sample	Temperature °C	s
1V	300	.8379
	25	.0075
1S	300	.8359
	25	.5351
1D	300	.8854
	25	.3802
2V	300	.8215
	25	.0062
2S	300	.8461
	25	.5452
2D	300	.8625
	25	.4063
3S	300	.2697
	25	.0061
3D	300	.8034
	25	.4174

FIG. 4.17 - 4.22
× 0.075 K

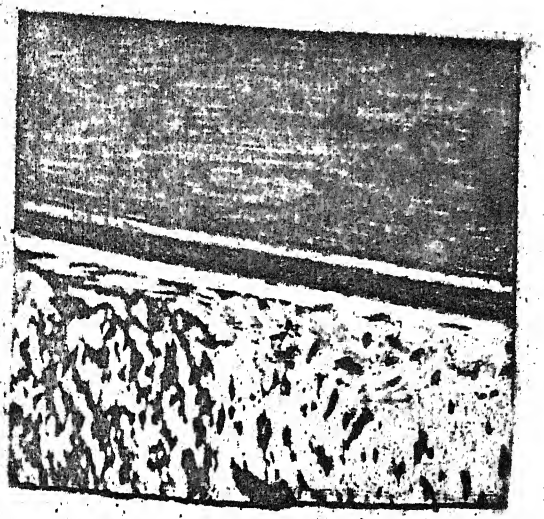

Sample 2S.3

FIG. 4.17

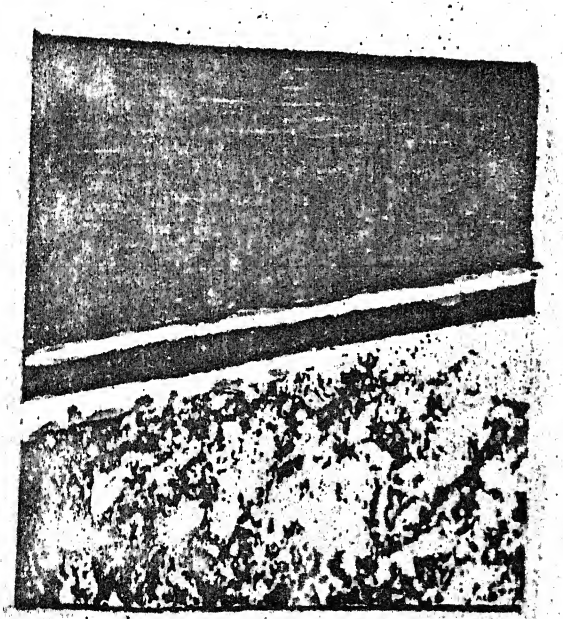

Sample 2S.2

FIG. 4.18

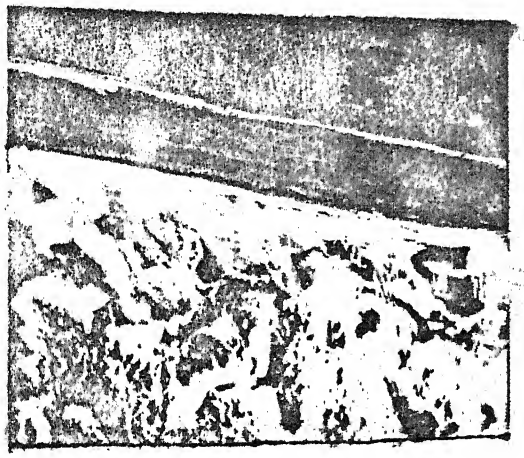

Sample 2S.1

FIG.4.19

Sample 2D.3

FIG. 4.20

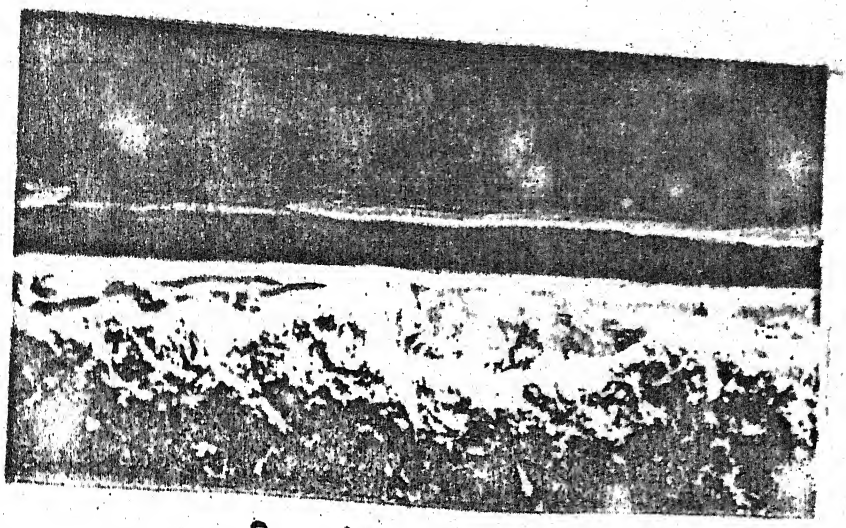

Sample 2D.2

FIG.4·21

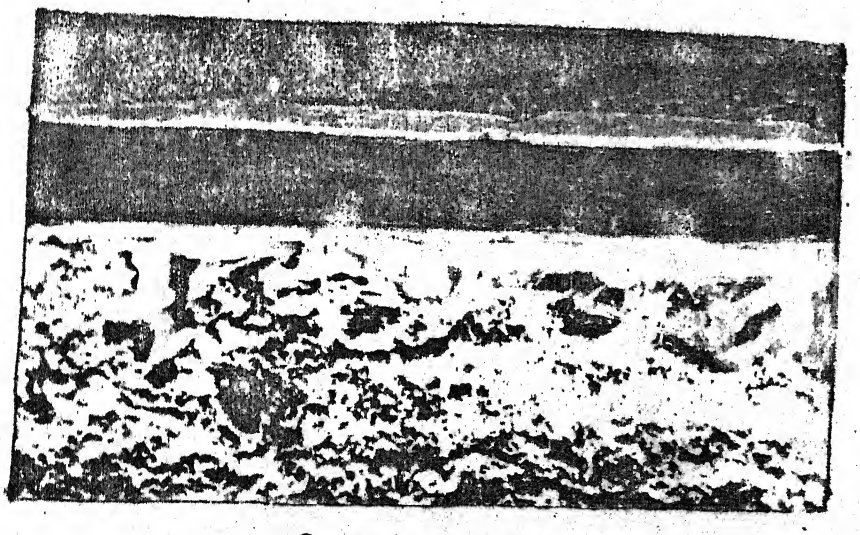

Sample 2D.1

FIG.4·22

TABLE 4.14

Thickness of Conducting Layer

Sample	Reduction time in hours	Reduction Temp. °C	Thickness in micron
2S	0.5	250	50
2S	1.0	320	60
2S	2.0	320	130
2D	0.5	250	60
2D	1.0	320	72
2D	2.0	320	160

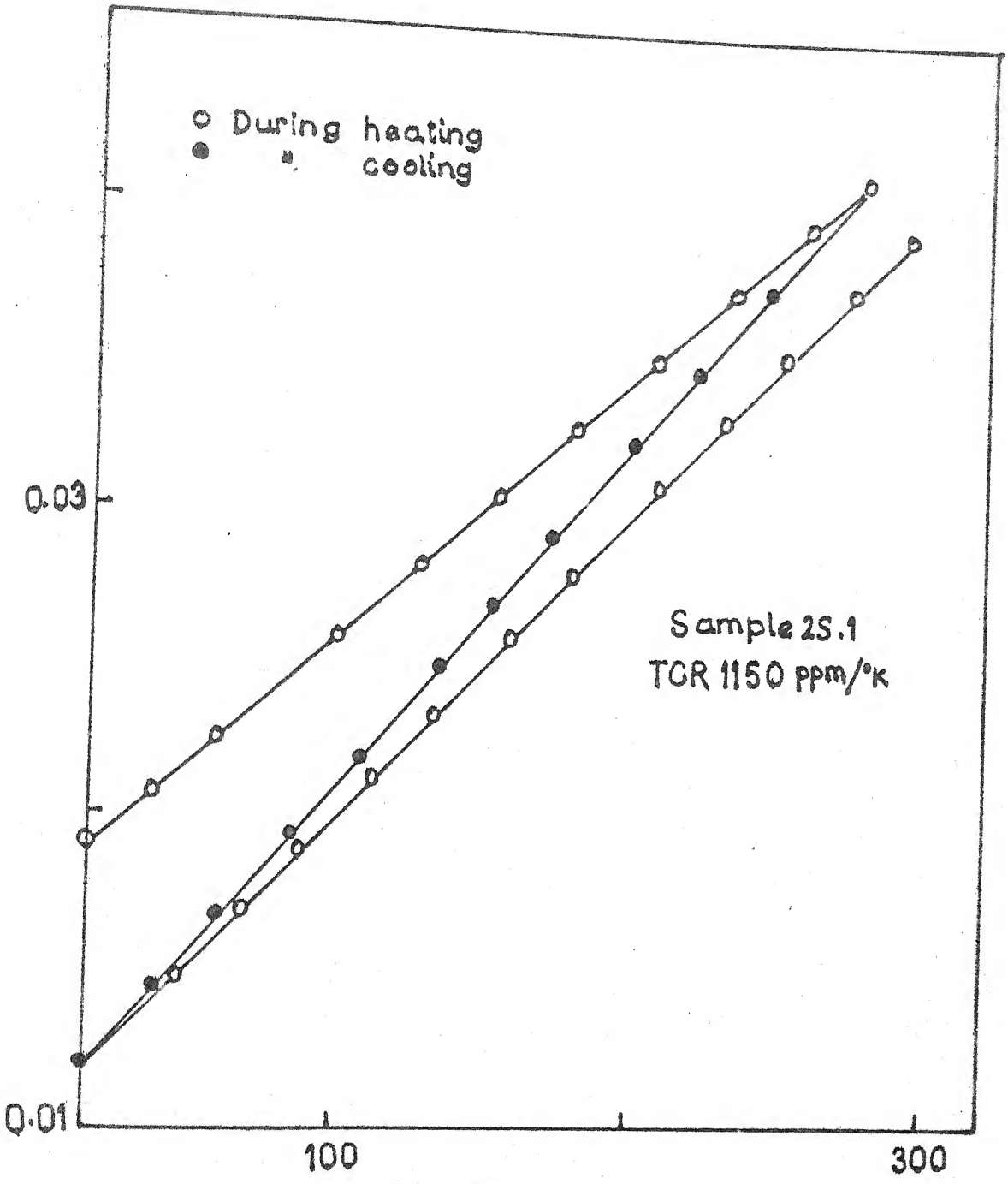
During heating
cooling
0.03
0.01
Sample 2S.1
TCR 1150 ppm/°K
100
300
Temp. (°C)

FIG. 4.23

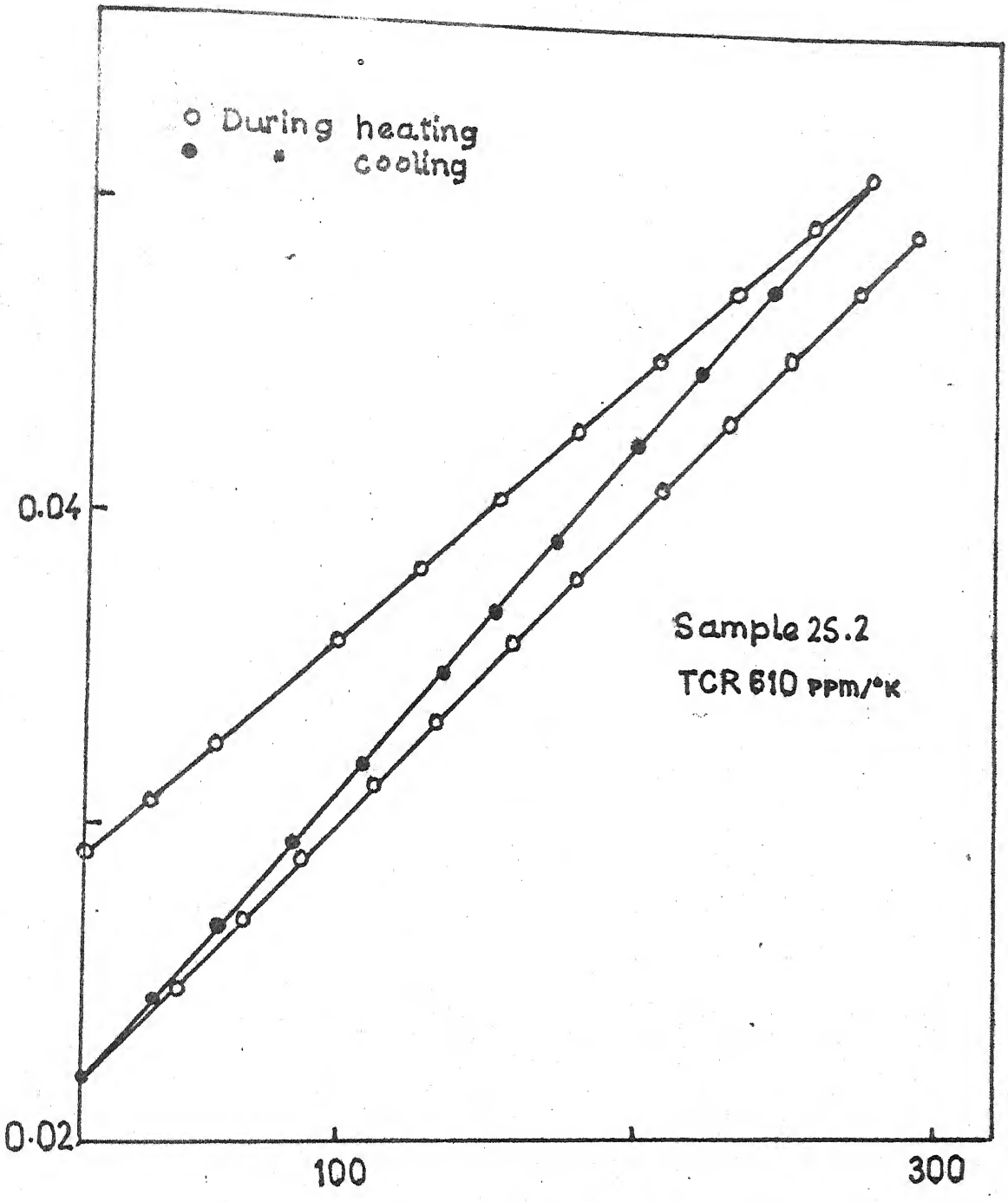
During heating
cooling
Sample 25.2
TCR 610 ppm/°K
0.04
0·02
100
300
Temp. (°C)

FIG. 4.24

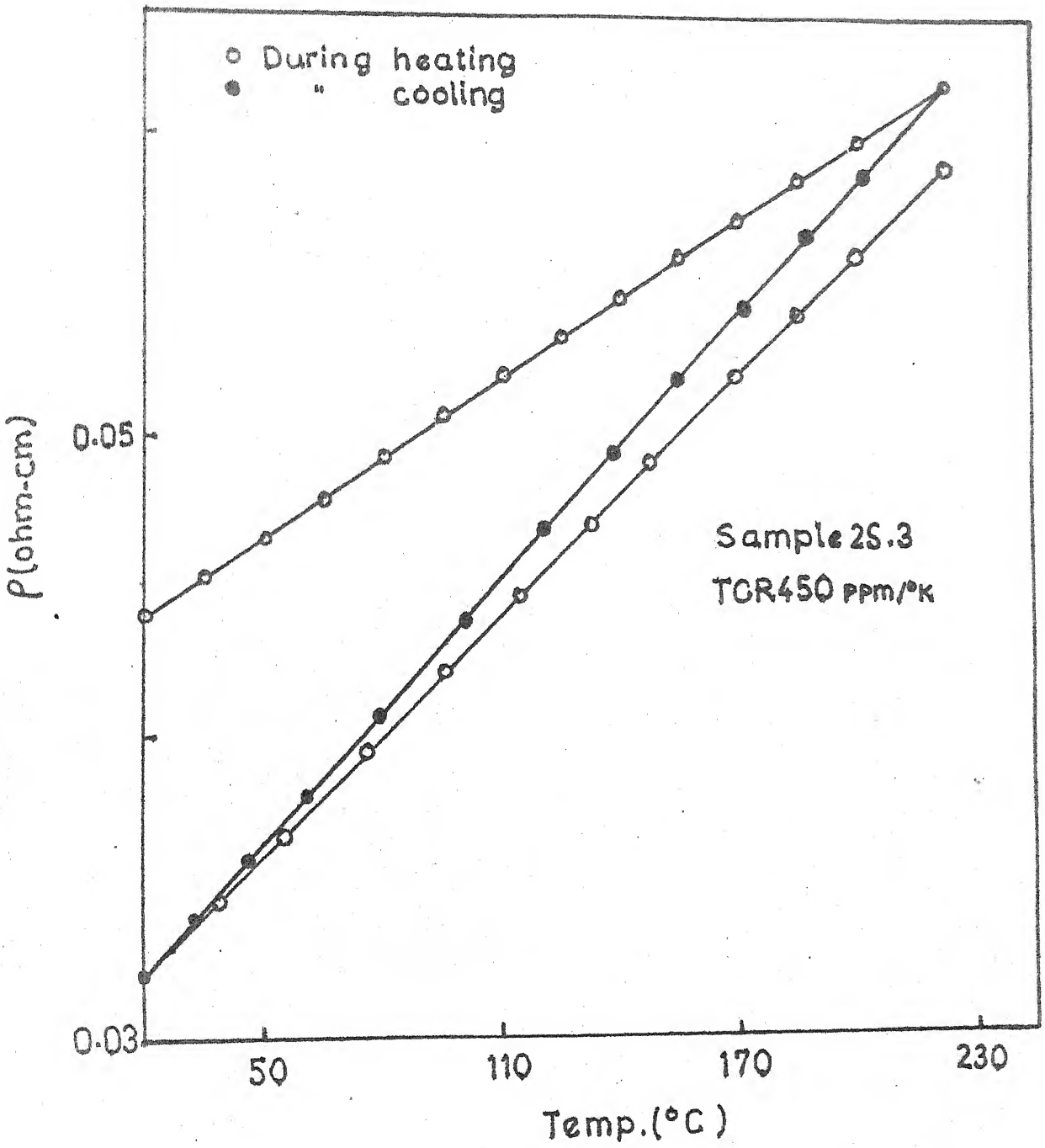
During heating
" cooling
Sample 2S.3
TCR450 ppm/°K
ρ(ohm-cm)
0.05
0.03
50
110
170
230
Temp.(°C)

FIG. 4.25

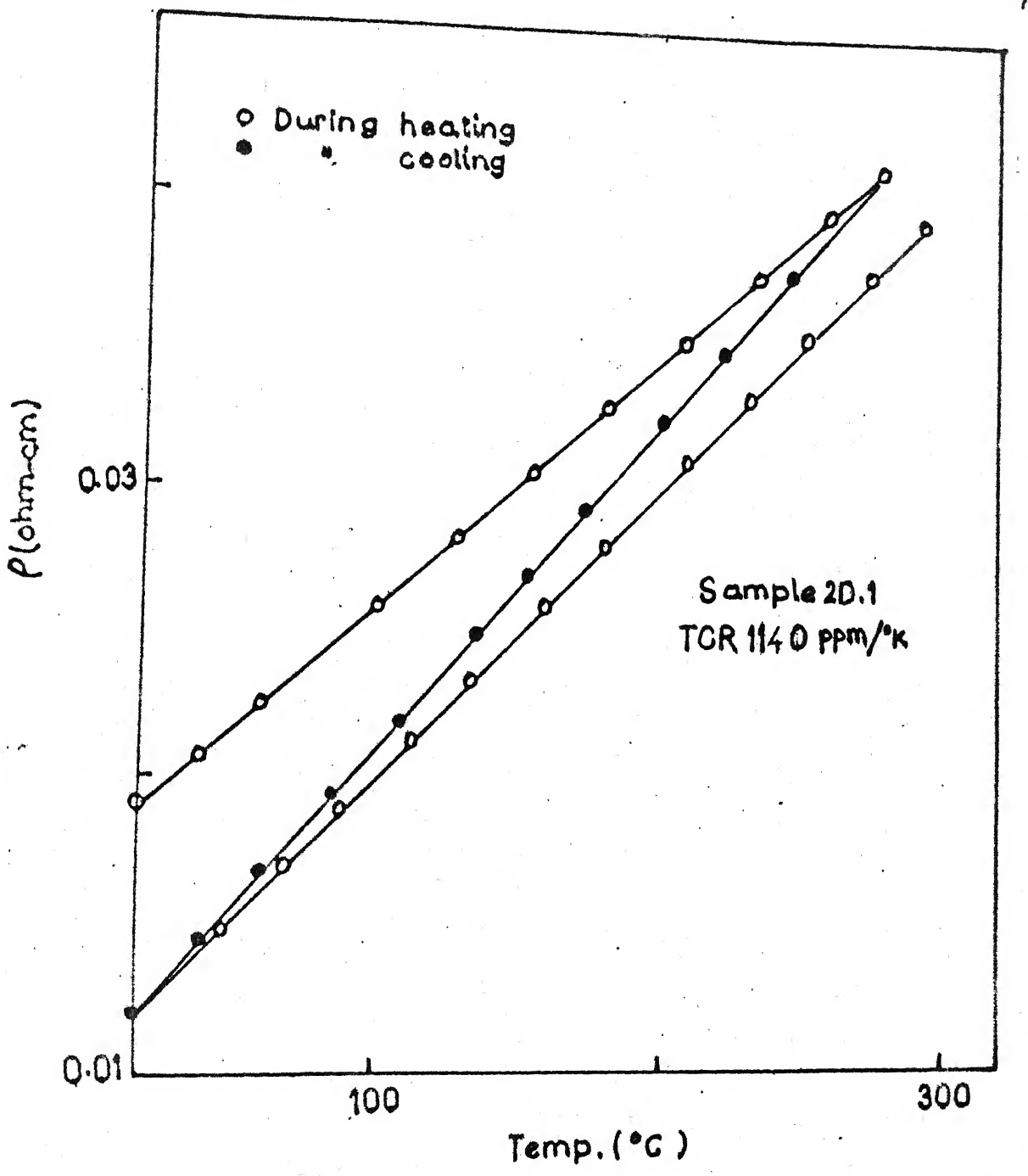
During heating
cooling
Sample 2D.1
TCR 1140 ppm/°K
ρ(ohm-cm)
0.03
0.01
100
300
Temp.(°C)

FIG. 4.26

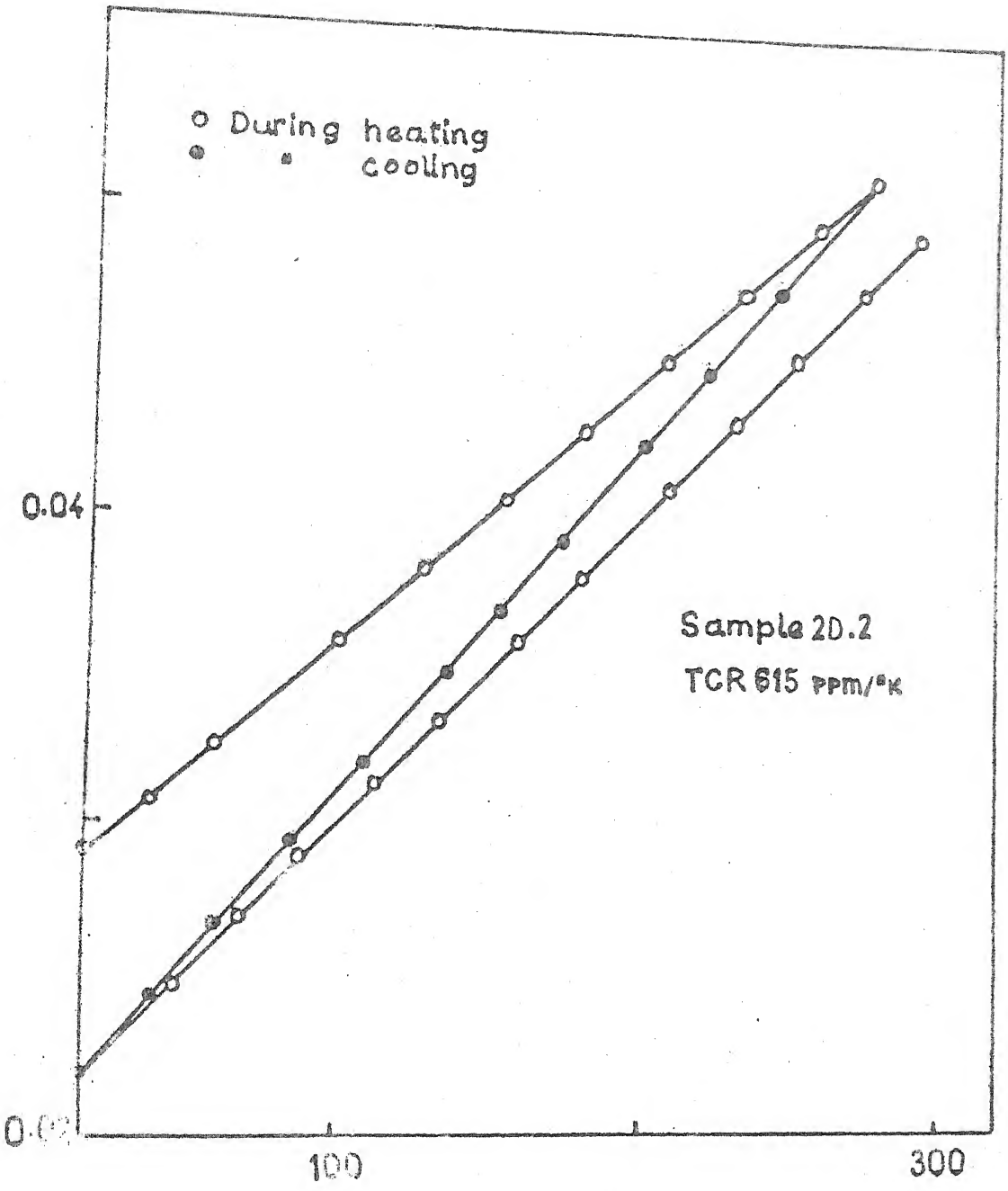
During heating
cooling
0.04
Sample 2D.2
TCR 615 ppm/°K
100
300
Temp. (°C)

FIG. 4·27

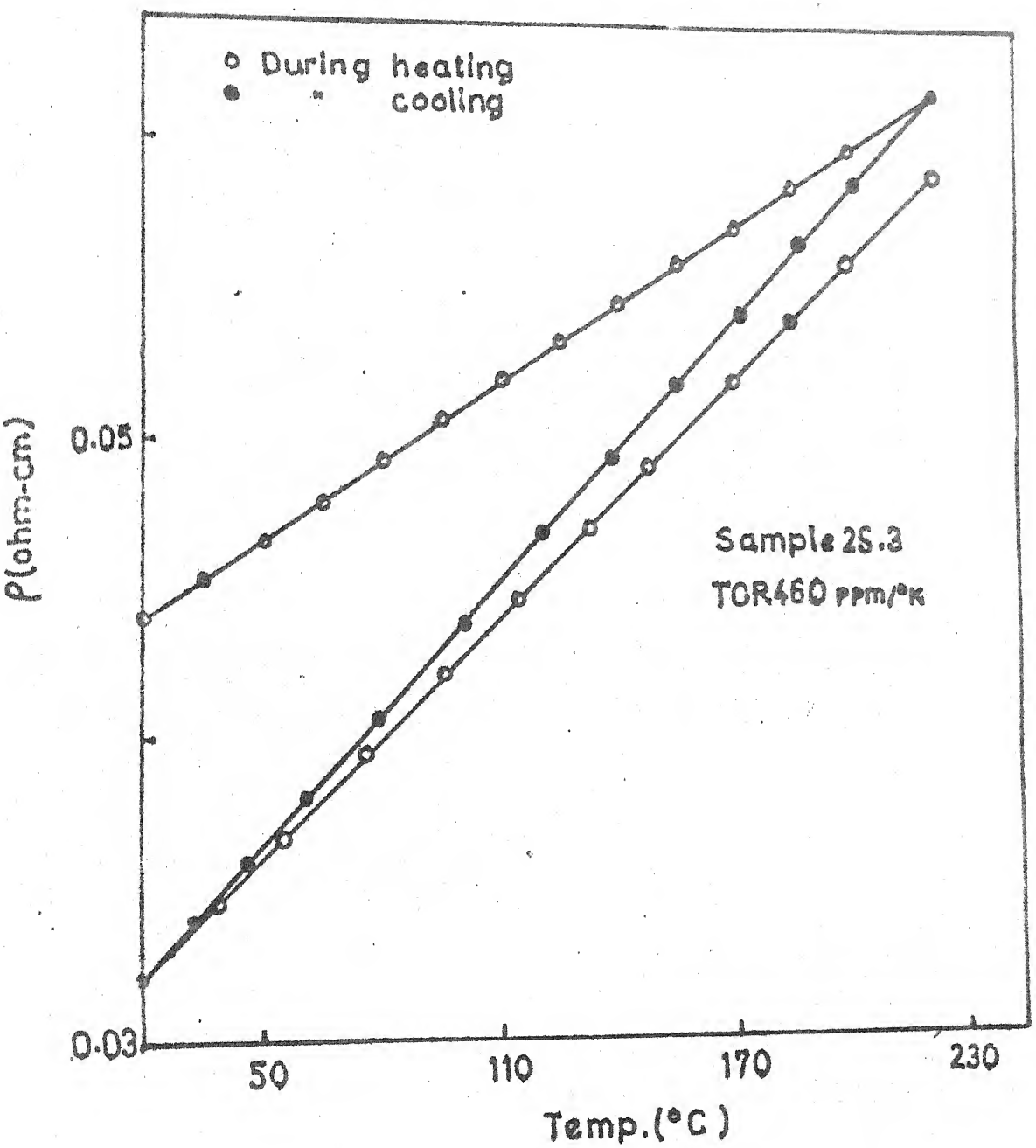
o During heating
● " cooling
Sample 2S.3
TCR460 ppm/°K
ρ(ohm-cm)
0.05
0.03
50
110
170
230
Temp.(°C)

FIG. 4.28

FIG. 4.29 - 4.34
× 0.8K

FIG. 4.29

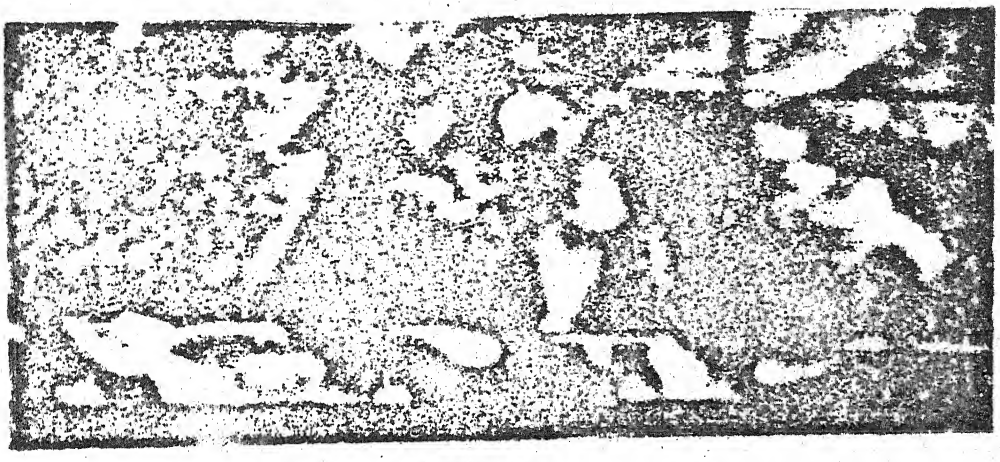

FIG. 4.30

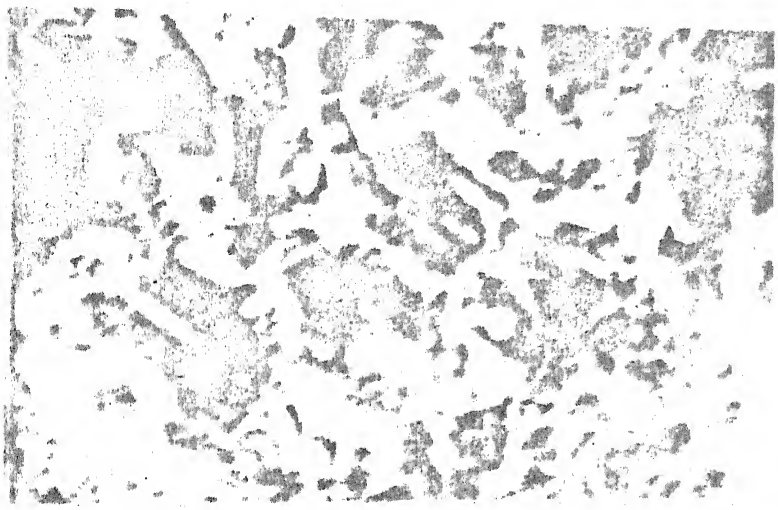

FIG. 4·31

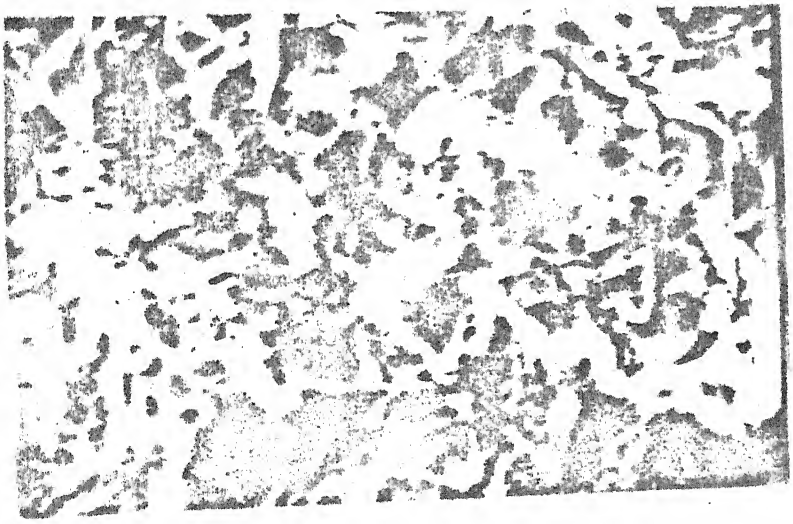

FIG. 4·32

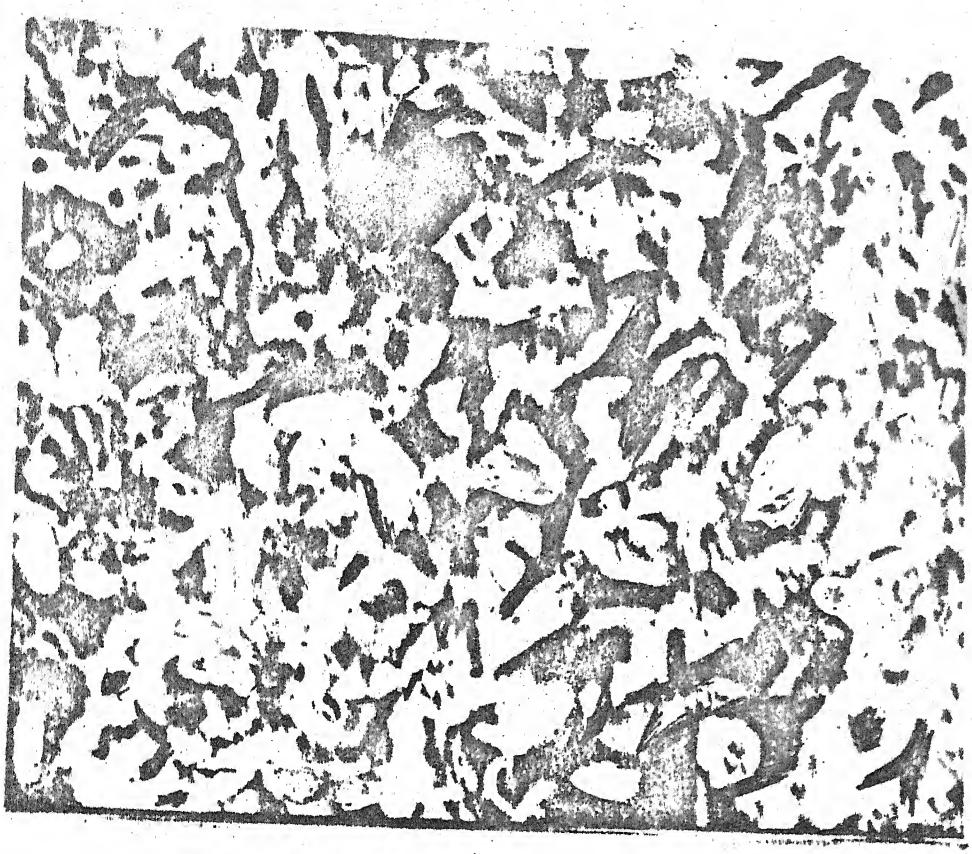

FIG. 4·33

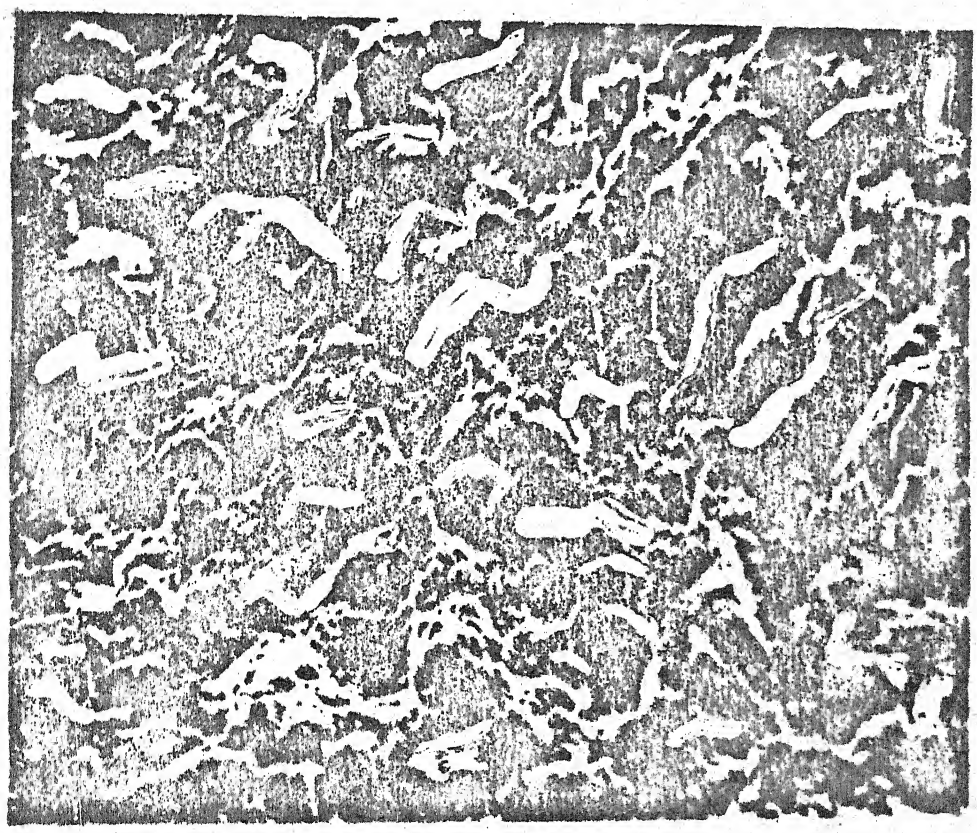

FIG. 4·34

TABLE 4.15

Microstructure data of Glass Ceramic Samples

Sample	Percent volume crystallisation
1S	55
1D	72
2S	53
2D	54
3S	60
3D	72

The data is very much in agreement with the information of X-ray data and resistivity data.

4.5 TRANSMISSION ELECTRON MICROGRAPH

The micrograph for 1V, 2V, 3V samples are given in figure 4.35, 4.36, 4.37. Interconnected phases are observed in all the samples.

FIG.4·35 - 4·37
×51 K

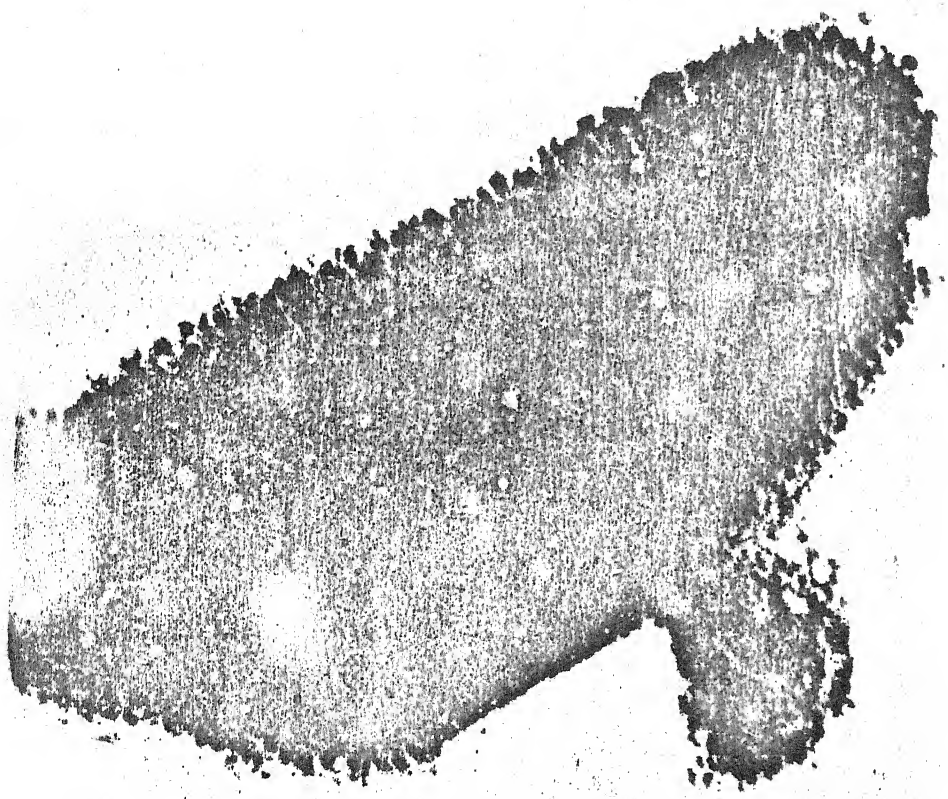

FIG. 4·35

CHAPTER 5

DISCUSSION

For samples 1 and 3 similar relative heights of the two exothermic peaks are observed but for glass 2 it is different. In glass 2 second exothermic peak is relatively higher.

First exothermic peak in glass 1 and 3 is identified as for zinc silicate crystals with a small amount of lithium phosphate crystals. Second phase is identified as lithium phosphate. The Li_2O content in glass 2 is maximum and this is the reason of the domination of lithium phosphate phase over zinc silicate phase in the first growth temperature.

Higher volume crystallisation in double heat-treated samples is due to the growth of second phase i.e. lithium phosphate phase except in glass 2. In glass 2 in first growth temperature the volume crystallisation is appreciably high. This is due to higher lithium content.

The conducting layer is observed to increase with reduction increase in temperature and time. For 2D samples longer ion exchange time is given and comparatively thicker conducting layer is obtained. This may be due to availability of higher Ag^+ ions.

For glasses 1 and 3, there is decrease in resistivity after the first heat treatment as the matrix becomes relatively richer in lithium content. After the second heat treatment there is again a rise in resistivity as lithium ions are expensed

for lithium silicate phase. For glass 2 the glass becomes less conducting even after first growth temperature as lithium silicate phase is given up. After the second growth temperature the amount of further growth is very less and so the resistivity does not change almost.

The AC resistivity does not change much with change in temperature.

The s values obtained from Table 4.13 for higher temperature is between 0.8 - 0.9. It is in accordance with Fritzsche[35] and can be concluded as for ionic hopping conduction.

The E values are found to be very large at high temperatures. This is due to the fact that higher energy is needed for creating vacancies as well as for the motion of ions into the vacancies. This again confirms the hopping of lithium ions.

The TCR valuesvary between 550 ppm/°K to 2500 ppm/°K. The TCR of silver metal is around 4000 ppm/°K. So as suggested by Chakravorty[8], the high surface conductivity is believed to be developed by the formation of interconnected chains of silver droplets. As the reduction temperature decreases the kinetics of Ag^+ ion reduction decreases and for shorter reduction time the number of silver atoms produced will be less. The decrease in temperature also causes the lowering of nucleation rate of silver atoms. For the shorter reduction duration the growth of silver particles will be small.

The net result is that smaller number of interconnected silver droplets will be formed, as a result of which the surface resistance increases.

The effect of measuring temperature is observed from the slope of the bulk resistance-temperature plots. The general trend is that the slope increases during cooling cycle of measurement. This change is believed to be due to the further precipitation of fresh silver droplets at the highest temperature of measurement. For samples reduced at lower temperature and for shorter duration the change of slope for the surface resistance versus temperature plots during heating and cooling cycles, is found to be more pronounced than that reported for samples reduced at higher temperatures. This difference can be explained by assuming that precipitation of silver particles occurs by migration of silver atoms to the stable nuclei. Thus at lower reduction temperatures even more silver atoms are available for generation of fresh silver droplets than those existing in samples reduced at higher temperatures.

With reference to previous work[33], by using hydrogen alone in reduction treatment, the bulk resistance has been lowered by ten orders of magnitude in a considerably shorter reduction time. In contrast to the use of the mixture of hydrogen and nitrogen gas, the use of hydrogen gas alone probably increases the kinetics of reduction of Ag^+ ions considerably.[10] So higher bulk conductivity is achieved.

The continuous change in slope in log ρ -1000/T plot for virgin samples cannot be properly explained. However, this may be attributed to the two interconnected phases present in the glasses.

CHAPTER 6

CONCLUSION

From the experimental studies, made on the glass ceramic samples of SiO_2-ZnO-Li_2O-P_2O_5 system the following conclusions are drawn:

(1) Zinc silicate crystals grow if the lithium oxide content is low.

(2) Due to the growth of zinc silicate the resistivity decreases.

(3) Due to the growth of lithium phosphate the resistivity increases.

(4) The conduction mechanism is ionic hopping.

(5) The thickness of the conducting layers has been found to be 130 micron for 6 hours of ion exchange and 3 hours of reduction at 300°C.

REFERENCES

1. D.Chakravorty, Preparation and Characterization of Materials, ed., C.N.R.Rao and J.M.Honig (Academic Press, London, in press).
2. H. Schulz, Glashiitte, 66, 685 (1936).
3. L.J. Dykstra and E.M. Meyer, U.S. Patent 2274955 (1942).
4. T.W.H. Ward, U.S. Patent 2280135 (1942).
5. R.L.Green and K.B. Blodgeet, J.Am. Ceram. Soc. 31, 89 (1948).
6. K.B. Blodgeet, J.Am. Ceram. Soc. 34, 14 (1951).
7. D. Chakravorty, U.K. Pat. Application No.41515/71, (French Patent No. 72/31218).
8. D. Chakravorty, J. Non-Cryst. Solids, 15, 191-198, (1974).
9. G.C.Das, T.K.Reddy and D. Chakravorty, J.Mat. Sc. 13, 3211 (1978).
10. G.C.Das, M.Tech. Thesis, I.I.T. Kanpur, January (1977).
11. D. Chakravorty, Appl.Phys. Lett. 24(2), 62 (1974).
12. D. Chakravorty and C.S. Murthy, J. Phys. D: Appl. Phys. 8, L162 (1975).
13. P. Hing and P.W. McMillan, J. Mat. Sc., 8, 1041 (1973).
14. G.C. Das, Ph.D. Thesis, I.I.T. Kanpur, January (1982).
15. S.D.Stookey, Brit. Pat. No. 635649, (1947).
16. R. Becker, Ann. Phys., 22, 128-140 (1938).
17. Z. Strand and R.W. Douglas, Phys. Chem. Glasses, Vol.14(2), April (1973).
18. D.G. Burnett and R.W. Douglas, Diss. Fara. Soc., 1970, No.50, 200-5.
19. D. Turnbull, J. Chem. Phys., 20: 411-424 (1950).
20. A.I. Berezhnoi, 'Glass-Ceramics and Photo-Sitalls', (1970).
21. S.D. Stookey, U.S. Patent No. 2515275 (1950).